Fisheries and Oceans Canada | Pêches et Océans Canada
Ecosystems and Oceans Science | Sciences des écosystèmes et des océans

Canadian Science Advisory Secretariat (CSAS)

Research Document 2024/013

Maritimes Region

Framework Assessment of Atlantic Halibut on the Scotian Shelf and Southern Grand Banks (NAFO Divisions 3NOPs4VWX5Zc)

S. Johnson[2], B. Hubley[1], S.P. Cox[2], C.E. den Heyer[1] and L. Li[1]

[1]Population Ecology Division
Bedford Institute of Oceanography
PO Box 1006
Dartmouth, Nova Scotia, B2Y 4A2

[2]Landmark Fisheries Research
Coquitlam, BC, Canada

February 2024

Canada

Foreword

This series documents the scientific basis for the evaluation of aquatic resources and ecosystems in Canada. As such, it addresses the issues of the day in the time frames required and the documents it contains are not intended as definitive statements on the subjects addressed but rather as progress reports on ongoing investigations.

Published by:

Fisheries and Oceans Canada
Canadian Science Advisory Secretariat
200 Kent Street
Ottawa ON K1A 0E6

http://www.dfo-mpo.gc.ca/csas-sccs/
csas-sccs@dfo-mpo.gc.ca

ISSN 1919-5044
ISBN 978-0-660-70059-5 Cat. No. Fs70-5/2024-013E-PDF

Correct citation for this publication:

Johnson, S., Hubley, B., Cox, S.P., den Heyer, C.E., and Li, L. 2024. Framework Assessment of Atlantic Halibut on the Scotian Shelf and Southern Grand Banks (NAFO Divisions 3NOPs4VWX5Zc). DFO Can. Sci. Advis. Sec. Res. Doc. 2024/013. iv + 58 p.

Aussi disponible en français :

Johnson, S., Hubley, B., Cox, S.P., den Heyer, C.E., et Li, L. 2024. Évaluation du cadre pour le flétan de l'Atlantique sur le plateau néo-écossais et dans le sud des Grands Bancs (divisions 3NOPs4VWX5Zc de l'OPANO). Secr. can. des avis sci. du MPO. Doc. de rech. 2024/013. v + 62 p.

TABLE OF CONTENTS

ABSTRACT

Atlantic Halibut (*Hippoglossus hippoglossus*) is a large sexually dimorphic flatfish and currently the most valuable groundfish species by landed weight on the Atlantic coast. The 2014 framework for Atlantic Halibut on the Scotian Shelf and Southern Grand Banks developed a statistical catch-at-length (SCAL) model that estimated historical biomass, fishing mortality, age–1 recruitment, and biological reference points. SCAL model outputs were then used to condition, or parameterize, an age-structured operating model used to evaluate the performance of alternative TAC interim procedures. This paper describes the spatially integrated statistical catch at length (SISCAL) model adapted for Atlantic Halibut, an update of the data and software, but not the basic structure of the SCAL model which was included here for comparison. The SISCAL model estimates the 2021 spawning stock biomass to be 31.1 kt, with 95% credible interval (25, 36), the highest estimated biomass in the time series. This stock has increased from a heavily depleted state observed in the 1990s. It appears to be benefiting from a recent period of high recruitment. Estimates of total and legal-sized (greater than 81 cm since 1994) biomasses are also at record levels. Recent exploitation rates have been consistent with the target level of the constant F harvest rule adopted in 2014, providing evidence of success. Estimates of natural mortality M were allowed to vary over the time series, with recent (2014–2021) estimates of M ranging from 0.128 to 0.143, for males and from 0.120 to 0.133 for females. We used SISCAL to condition an updated operating model, estimate MSY-based reference points and test a suite of candidate management procedures using closed-loop simulations against Atlantic Halibut fishery management objectives.

INTRODUCTION

Atlantic Halibut (*Hippoglossus hippoglossus*) is a large sexually dimorphic flatfish and currently the most valuable groundfish species in Atlantic Canada There are two Atlantic Halibut management units in Canada, the Scotian Shelf and southern Grand Banks (Northwest Atlantic Fisheries Organization [NAFO] Divisions 3NOPs4VWX5Zc) and the Gulf of St. Lawrence (NAFO 4RST), defined based primarily on tagging studies (McCracken 1958, Bowering 1986, Stobo et al. 1988) and differences in growth rates (Neilson and Bowering 1989). Further differences within the Scotian Shelf and Southern Grand Banks, between NAFO 3NOPs and 4VWX5Zc, were identified in the size composition from the catch in these areas and lead to the adoption of an areas as fleets approach to the assessment of the stock (Cox et al. 2016).

The initial (1998) total allowable catch (TAC) for the Scotian Shelf and Southern Grand Banks was set at 3,200 t, which was subsequently reduced to less than 1000 t as the quota was not caught. In 1994, a minimum size limit of 81 cm was established. Since 1999 the TAC and landings have increased five-fold. Prior to 2010, science advice was provided based on the Fisheries and Oceans Canada (DFO) research vessel (RV) abundance indices and catch per unit effort (e.g., Perley et al. 1985, Zwanenburg et al. 1997). In 1998, industry, working with DFO, initiated a fixed station longline Halibut survey to provide a fishery-independent index of exploitable biomass throughout the management unit. In 2010, a length-based age-structured assessment model was adopted (Trzcinski et al. 2011, Trzcinski and Bowen 2016).

The 2014 assessment framework for Atlantic Halibut on the Scotian Shelf and Southern Grand Banks developed new methods for monitoring stock size and productivity (Cox et al. 2016). The framework evaluated the long-term performance of a range of TAC and constant F harvest strategies via closed-loop simulation. The simulations were conditioned on statistical catch-at-length (SCAL) model estimates of historical Atlantic Halibut biomass, fishing mortality, recruitment, and biological reference points, and were projected forward to evaluate the risks of alternative interim procedures for setting TAC. Based on the science advice, since 2014 the Atlantic Halibut TAC has been set based on a constant fishing mortality F = 0.14 strategy applied to the index of exploitable biomass from the Industry-DFO Halibut Longline Survey.

Here, we present an updated SCAL model run and describe a spatially integrated statistical catch at length model adapted for Atlantic Halibut (SISCAL-AH), which is an update of the data and software, but has the same basic structure as the SCAL model. We used SISCAL to estimate MSY-based reference points, condition an updated operating model and test a suite of candidate management procedures using closed-loop simulations against Atlantic Halibut fishery management objectives. The management objectives and candidate procedures were developed through consultations with Atlantic Halibut fishing industry.

DATA INPUTS

A review of the data inputs for this model, including biological parameters, ecosystem considerations, landings, indices of abundance, catch composition and mortality estimates, was conducted at a CSAS process Nov 23–26, 2021 (Li et al. In press). New ageing data have been collected and a new growth model is used (Zheng et al. In prep.[1]).

[1] Zheng, N., Perreault, A.M.J., Li, L., Hubley, B., den Heyer, C.E., and Cadigan, N.G. In preparation. A Spatiotemporal Richards-Schnute Growth Model for Atlantic Halibut (*Hippoglossus hippoglossus*) on

LANDINGS

The two main gear types that land Atlantic Halibut are otter trawl (OT) and longline (LL) gears, with longline being the predominant type in recent years. The fishery data (landings and catch composition) were assembled separately for NAFO 3NOPs and 4VWX5Zc. Differences in the catch composition between these areas indicate a difference in the availability of certain size fish and thus differing selectivity for each area and gear type. Therefore, each area and gear type combination are treated as separate fleets in the model (LL3, LL4, OT3 and OT4), with annual landings data for the four fleets presented in Table 1.

INDICES OF ABUNDANCE

The SISCAL model was fit to three fishery independent indices of abundance (Figure 1). The stratified mean number of Atlantic Halibut per tow in the Maritimes Summer Ecosystem Research Vessel Survey (RV_4VWX) begins in 1970. The RV survey generally catches smaller Atlantic Halibut (< 81 cm) and is the main indicator of recruitment to the fishery. It runs from 1970 to 2020 but mechanical issues in 2018 limited the survey in that year to 4X. The mean number of Atlantic Halibut per tow in 4X in 2018 (0.53) was in-between the mean number of Atlantic Halibut per tow in 4VWX in 2017 (0.62) and 2019 (0.41), so removing this data point would not have any major impact on the model results. The fixed station portion of the Industry-DFO Halibut Longline Survey begins in 1998 and stations were initially allocated based on commercial fishery catch rates with more stations in higher catch rate areas, as a result the survey also was focused more on 4VWX5Zc, with fewer stations proportional to area in 3NOPs. Since 2017, 100 of the most frequently fished fixed stations in the time series (1998–2015) that also provided good coverage of the survey area have continued to be fished alongside the new stratified random stations to calibrate the new survey. The mean weight of Atlantic Halibut caught per 1000 hooks in these 100 stations make up the fixed station portion of the Industry-DFO Halibut Longline Survey index that is used in the model. In 2017, a stratified random survey with standardized fishing protocols, expanded geographic coverage and increased data collection was introduced. The Stratified Random portion of the Industry-DFO Halibut Longline Survey area is divided into 5 spatial strata (4X5YZ, 4W, 4V, 3P, 3NO), each with 3 depth zones (30–130 m, 131–250 m, 251–750 m). One hundred and fifty stations were allocated proportional to area in the 15 strata, with 3 extra stations added to the smallest strata that had only 2 stations initially. The stratified mean weight of Atlantic Halibut caught per 1000 hooks in these 153 stations make up the stratified random portion of the Industry-DFO Halibut Longline Survey index. The stratified random index covers the whole stock area and thus is somewhat lower than the fixed station index. We also attempted to fit the NAFO area 3 RV survey index, but the increase in this index was not able to be matched by the model survey biomass (Appendix A), so it was not retained in the model.

LENGTH COMPOSITION

Length composition data from the fishery comes from both port sampling and at-sea observers and are discussed in Li et al. (in press). Notably Atlantic Halibut can only be sexed by looking at the gonads, so there is no sex assignment for discarded or undersized fish. At-sea observers generally collect sex information for legal-sized Atlantic Halibut but, as Atlantic Halibut are landed gutted, sex information in port sampling data are less frequently collected. These data were combined to form the length compositions for each fleet and the model was fit to males,

the Scotian Shelf and Southern Grand Banks (fit to preliminary data). DFO Can. Sci. Advis. Sec. Res. Doc.

females and the overall (males, females and unsexed) length composition. The SISCAL model is also fit to length composition data collected during the three abundance index surveys, which also record sex information when available (Figure 2).

MODEL DESCRIPTION

STATISTICAL CATCH AT AGE AND LENGTH MODEL

The SISCAL model is an age- and sex-structured population dynamics model fit to fishery-independent indices and length compositions, and fishery landings and catch-at-length data. Landings and length compositions are split by gear type (longline and otter trawl) and area (NAFO areas 3NOPs and 4VWX5Zc), making the SISCAL model a spatially implicit areas-as-fleets model. Model notation is given in Table 2 and population dynamics process model and statistical model equations in Tables 4 and 5, respectively.

Model parameters (Table 3, P.1–P.4) are partitioned into four subsets consisting of leading parameters Θ^{lead}, nuisance catchability and observation model variance parameters Θ^{cond} estimated conditionally on leading parameter values, fixed parameters Θ^{fixed} for maturity-at-age parameters and recruitment deviation and natural mortality random walk deviation standard errors, and finally prior distribution hyperparameters Θ^{prior}.

SISCAL MODEL STATE DYNAMICS

Unfished equilibrium recruitment (EQ.4) and numbers-at-age (EQ.5) are derived via spawning biomass per recruit (EQ.3), which is itself a function of time-averaged natural mortality, weight-at-age, maturity-at-age (EQ.1), and unfished equilibrium survivorship-at-age (EQ.2).

Annual recruitment (occurring on the first day of the year) is assumed to follow a Beverton-Holt stock-recruitment function parameterized via stock-recruitment steepness h, unfished spawning stock biomass B_0, recruitment process error deviations ω_t, and annual natural mortality rates $M_{x,t}$. The time-varying mortality rate starts with an initial estimated $M_{x,1}$ in 1970 and then proceeds via a random walk with the same jumps applied to both sexes (Table 3, EQ.2).

Age- and sex-class abundances are initialised in a fished state by estimating an initial recruitment parameter R_{init} and assuming an equilibrium age structure (Table 3, NEQ.1), effectively scaling the population to a proportion of unfished. Initial recruitment is used over initial abundance-at-age because the uncertainty is too great to estimate the latter without catch-at-age data.

Selectivity-at-age for each sex and fleet is modeled as a logistic function of length-at-age (Table 3, S.1). Selectivity is asymptotic (logistic) for the long line fleets, and dome-shaped (double asymptotic) for the otter trawl fleets. All fleets use the same parameters for the ascending limb: length-at-50% selectivity $s_g^{50,A}$ and the difference between length-at-50% and length-at-95% selectivity $s_g^{Step,A}$. For otter trawls, there are additional two descending limb parameters, length-at-95% selectivity and length-at-50% selectivity. Length-at-95% selectivity for the descending limb is modeled as a step from length-at-95%, i.e., $s_g^{95,D} = s_g^{95,A} + s_g^{Step,1,D}$ selectivity for the ascending limb, and descending limb length-at-50% selectivity a further step from length-at-95%, i.e., $s_g^{50,D} = s_g^{95,D} + s_g^{Step,2,D}$, thereby ensuring the descending limb is always to the right of the ascending limb, which reduces the sharpness of the peak in selectivity. Selectivity-at-length is converted to sex-specific selectivity-at-age via a simplified two-sex Richards-Shnute growth model, which accounts for gear size-selectivity and length stratified sampling (G.1) (Zheng et al. In prep.[1]).

Commercial removals by longline (LL) and otter trawl (OT) fisheries in both NAFO areas 3 and 4 are represented as discrete fisheries occurring around halfway through the year at a fractional time step δ_g (Table 3, C.1–C.9), where $0.47 < \delta_g < 0.52$. Fish are removed from each area by converting landings to total catch by scaling by the probability released and the proportion of vulnerable biomass at age (C.6), which is then converted to total caught numbers-at-age via the mean weight-at-age (C.7). Total caught numbers are then removed from the vulnerable numbers-at-age (C.8), and removals of sub-legal fish are based on the discard mortality (C.9). Annual exploitation rates for total landings U_t and each commercial fleet $U_{g,t}$ are calculated as the ratio of landed legal-sized catch to the total legal biomass (Table 3, C.10).

It is commonly assumed that reproduction is proportional to mass and a linear relationship has been applied to many groundfish stock assessments, including Pacific halibut (Stewart and Hicks 2019). Recent studies show that the hyperallometric reproduction could result in higher yields (Marshall et al. 2021). An exploration positive allometry in the fecundity relationship is presented in Appendix B.

OBERVATION MODELS, LIKELIHOOD FUNCTIONS, AND PRIORS

Temporal variation in Atlantic Halibut stock abundance and population composition are monitored via a DFO RV survey in area NAFO area 4VWX, and DFO-industry collaborative longline Halibut survey (HS) which covers the entire management unit (NAFO 3NOPs4VWX), the latter of which is currently transitioning from a fixed survey design to a stratified random design. Length compositions are also collected by both surveys and all four commercial fleets (OT and LL in NAFO areas 3 and 4).

SURVEY INDEX OBSERVATIONS

Survey indices are assumed to be linear (i.e., no hyperstability or hyperdepletion) in the quantity that they are indexing, which is total vulnerable numbers for the RV survey, and vulnerable biomass for both the fixed station and stratified random HS (Table 4, O.1). Catchability and observation error variance parameters are estimated as conditional maximum likelihood estimates.

LENGTH COMPOSITION OBSERVATION MODELS

Proportion-at-length (i.e., length composition) observations are modeled in 5 cm bins via a logistic-normal likelihood function (Schnute and Haigh 2007; Francis 2014), with expected values calculated as proportions of the catch-at-length (Table 4, O.2; Figure 3). Annual length data samples for both sexed and unsexed samples were weighted relative to the average annual sample size for each fleet/sex combination (L.4), and fleet-specific lag-1 auto-correlation matrices were estimated for length composition residuals (L.1). To avoid zeroes in the length composition data, a tail-compression procedure was applied that combined data from length bins with less than 2% of the samples with neighbouring length bins (to the right) that were above that threshold, creating a variable number of bins at each time step (L.5). Fleet and sex-specific length sampling error standard deviations were conditionally estimated as nuisance parameters (L.7).

OBJECTIVE FUNCTION AND OPTIMISATION

The SISCAL objective function is proportional to the negative log posterior density function and defined as the sum of the negative log likelihood function values for observed data (Table 4, NLL.5, L.8 and F.4), negative log prior densities for process errors (P.1–P.2), and priors on other leading parameters (P.3–P.7).

The SISCAL model was specified in Template Model Builder (TMB), and the objective function was optimised via the nlminb() function in the R statistical package (R core team 2015; Kristensen et al. 2015). Model parameters were considered converged when the maximum gradient component of the likelihood surface had absolute value less than 10^{-2}, and the Hessian matrix was positive definite. Bayes posterior distributions were then sampled as 4 independent chains of 1,000 samples each using Hamiltonian Monte-Carlo (Monnahan and Kristensen 2018), or No U-turn Sampling. Hamiltonian Monte-Carlo differs from Markov-Chain Monte-Carlo by minimizing the auto-correlation between successive posterior samples, thereby producing a mixed model posterior sample with lower absolute sample sizes and little or no thinning (Monnahan et al. 2017).

HARVEST STRATEGY SIMULATIONS

The ms3-HAL closed-loop simulation package is conditioned to the SISCAL-AH operating model as described above, integrating over parameter uncertainty by sampling 100 random sets of parameter values from SISCAL-AH Bayesian posteriors. The dynamics of the ms3-HAL simulations match the SISCAL-AH time series of biomass, recruitment, and catch exactly over the historical period (Figure 19), so the model equations in Table 2 are not reproduced.

The ms3-HAL operating model provides a practical and realistic representation of Atlantic Halibut stock dynamics, fishery harvesting processes, and fishery monitoring data so that non-linear stock dynamics, time-lags, and data uncertainties can be accounted for in annual TAC advice. These processes, along with size limit regulations and at-sea release protocols (i.e., discard induced mortality) interact to determine short- and long-term performance of fishery harvest strategies with respect to fishery objectives (Table 5). Performance relative to fishery objectives (Table 6) under closed-loop simulation provides a robust approach to assessing fishery compliance with national fishery policies, such as the Sustainable Fisheries Framework and Fish Stocks Provisions.

A total of 18 Atlantic Halibut candidate management procedures were evaluated in closed-loop simulation. The first two management procedures are the no fishing procedure **NoFish** and the current management procedure **conF_0.14_15%**, which are meant to show baseline model dynamics. The remaining 16 management procedures are a factorial combination of 4 factors with 2 levels each (Table 7). Those factors are

1. Survey, and associated control points and catchability parameters (Figure 1, Table 8)
    a. Fixed station Atlantic Halibut survey
    b. Stratified random Atlantic Halibut survey
2. Harvest control rule:
    a. rampedFmsy: A standard Precautionary ramped harvest control rule, with 2 control points at survey biomass limit reference point (LRP) (0.4 B_{MSY}) and the upper stock reference (0.8 B_{MSY}) and a 100% TAC change limit at all biomass levels (Table 8, Figure 20);
    b. artic1.2Fmsy: An articulated harvest control rule, with three control points at the LRP, the USR, and at 1.2 B_{MSY}, with a sliding inter-annual TAC change limit going from 15% at the USR to 100% at the LRP (Table 8, Figure 21).
3. Legal size limit of 81 cm (**sl81**) or 86 cm (**sl86**) (Figure 22).
4. Release of whales: With (**rel170**) or without (**keep170**) a voluntary release of large (170+ cm) Atlantic Halibut, where an 80% release rate is applied to reflect that the action is voluntary (Figure 23).

Management procedure labels are a concatenation of the factor levels, e.g., **HSfix_artic1.2Fmsy_sl81_rel170** is the management procedure that uses the fixed station survey biomass to set target fishing mortality rates using the artic1.2Fmsy harvest control rule, has a legal size limit of 81 cm, and an 80% release rate on fish larger than 170 cm long.

At each time step t, all management procedures (except for NoFish) set TACs according to the following steps

1. Compute the 3-year average of (fixed or stratified random) Atlantic Halibut survey index I_t;
2. Compute the estimated survey biomass from the 3-year average index via

$$\widehat{B_t} = \frac{I_t}{\underline{q}};$$

3. Calculate the target fishing mortality rate F_t from the appropriate harvest control rule (Table 9). If the management procedure is **conF_0.14_15%**, then F_t = 0.14;
4. Compute the proposed $TAC'_t = (1 - e^{-F_t})B_t$;
5. Apply any interannual TAC change limit Δ_t defined by the management procedure either 0.15 for **conF_0.14_15%**, or according to the sliding scale for the articulated1.2Fmsy rule (Table 9), i.e.,
   a. If $TAC'_t > (1 + \Delta_t)TAC_{t-1}$, then $TAC_t = (1 + \Delta_t)TAC_{t-1}$;
   b. If $TAC'_t < (1 - \Delta_t)TAC_{t-1}$, then $TAC_t = (1 - \Delta_t)TAC_{t-1}$;
   c. Otherwise, $TAC_t = TAC'_t$

The final TAC_t for each year is then allocated among the 4 commercial fleets according to allocated proportions in 2021 (Table 5). Catches are removed from the population as in the SISCAL-AH model, where fleets are assumed to take catch in one discrete pulse in the middle of the fishing year, before and after which half of the natural mortality is applied.

CLOSED-LOOP SIMULATION ALGORITHM FOR EVALUATING HARVEST STRATEGIES

The following algorithm was used to simulate performance of alternative management procedures over two generations (28 years):

1. Define the Atlantic Halibut candidate management procedure based on (i) a three-year moving average of DFO-Industry Atlantic Halibut survey biomass, (ii) a harvest control rule, (iii) a size limit regulation, and (iv) a voluntary release option;
2. Initialize ms3-HAL for the 1970–2021 period based on a SISCAL-AH posterior draw
3. Project the operating model population and Atlantic Halibut fishery into the future, one time step at a time, and
   a. Generate the new fixed station and stratified random Atlantic Halibut survey biomass indices and landed catch for each fleet, append to existing Atlantic Halibut observation data set;
   b. Apply the harvest decision rule defined above and generate a TAC;
   c. Update the ms3-HAL operating model population dynamics given the total natural mortality, removals due to fishing, and size-based discarding generated by the final

landed catch limit, allocation among fisheries, size-based discarding, and new recruitment;

4. Repeat steps 3a–3c until the 28 time steps have passed and the simulation ends.
5. Repeat steps 2–4 for 100 random replicates, each of which draws a new SISCAL-AH posterior sample, and new sequence of random recruitment process and survey observation errors in the projection period.

PERFORMANCE METRICS

Candidate management procedures (MP) are quantitatively evaluated based on a suite of conservation and catch performance metrics. Each performance metric is defined based on Atlantic Halibut fishery management objectives (Table 5). The limit reference point B_LIM was defined as 0.4 B_{MSY} = 5,300 t based on the new SISCAL-AH model estimates of Atlantic Halibut biological reference points, and the upper stock reference (USR) was defined as 0.8 B_{MSY} = 10,600 t. Performance metrics (and their associated objectives) are:

- **Objective 1 - Probability that Biomass is below the LRP (pLRP):** The mean proportion of simulation replicates and years that spawning biomass is below the LRP of 6,500 t over 2 generations (28 years);
- **Objective 2 - Probability of decline (pDecline):** The proportion of simulation replicates that decline (on average) over 1 generation (14 projection years);
- **Objectives 3 and 4 - Mean Absolute Annual Change in catch over 10 years (mAAC10):** Mean interannual absolute change in TACs for 2022–2031.
- **Objective 5 a) - Average Catch over 10 years (avgC):** Median average catch for 2022–2031;
- **Objective 5 b) - Duration of peak resource utilization (nPeak):** Median number of projection years before TACs drop below 120% of MSY (2,640 t);
- **Objective 5 c) - Average Annual Variation in catch over 28 years (mAAC2gen):** Mean interannual absolute change in TACs for 2022–2049.

Although they are not related to any Atlantic Halibut fishery objectives, the following additional performance metrics are included:

- **Probability that biomass is in the healthy zone at end of simulation (pHealthy):** Mean proportion of simulation replicates and years (after 2040) where biomass is above the healthy zone boundary of 0.8 B_{MSY} (requested for compliance with Fish Stock Provisions and Sustainable Fisheries Framework);
- **Probability that biomass is above a target reference point (pTarget):** Mean proportion of simulation replicates and years (after 2040) where biomass is above a proposed target reference point of B_{MSY};
- **Probability of overfishing (pOverfish):** Mean proportion of simulation replicates and years where legal harvest rate is above U_{MSY};
- **Mean legal harvest rate above U_{MSY} (mU_Overfish):** Mean harvest rate in years/replicates where $U > U_{MSY}$.

The mathematical description of each performance metric is given in Table 6.

RESULTS

The 2014 framework model (SCAL) and SISCAL include similar dynamics of Atlantic Halibut sex-specific growth, mortality, and at-sea discarding of under-sized fish in the four main fisheries. An overall picture of the SISCAL model showing biomass, recruitment and harvest rate estimates are displayed in Figure 4.

FITS TO ABUNDANCE AND LENGTH COMPOSITION DATA

The SISCAL model captured the main features of the Maritimes Summer Ecosystem Research Vessel Survey abundance, the fixed station Atlantic Halibut survey biomass and the stratified random Atlantic Halibut survey biomass (Figure 5). Survey standard errors estimated from these fits were 0.23, 0.19 and 0.11, respectively, which are quite reasonable for fishery-independent survey data.

The SCAL model followed three periods of increased survey biomass in the Maritimes Summer Ecosystem Research Vessel Survey, the first between 1974 and 1983, the second between 1987 and 1994 and the third that began in 2004. Although both the early peaks result from periods of above-average recruitment, the second increase did not materialize into exploitable or spawning stock biomass (Cox et al. 2016). The SISCAL model, with time-varying natural mortality, estimates higher natural mortality during this period and has improved fit to the survey index (Figure 6). Recent estimates of M are below the prior of 0.145, but overall are similar with slightly higher values for males (Figure 7). Estimates of M between 2014–2021 range from 0.119 to 0.137, for males and from 0.111 to 0.128 for females.

Information about length-based selectivity is mainly obtained via SISCAL model fits to length composition data (Figure 8). Length-based selectivity curves estimated for each fleet and index of abundance are shown in Figure 9. Larger size selectivity is estimated in NAFO 3 fleets, where larger Atlantic Halibut are found. The stratified random portion of the Industry-DFO Halibut Longline Survey also selects for larger Atlantic Halibut when compared to the fixed station portion, which likely also reflects the higher proportion of sets in NAFO 3.

ESTIMATES OF ABUNDANCE, RECRUITMENT, AND EXPLOITATION

The SISCAL model predictions of spawning stock biomass for 1970–2021 show that the Atlantic Halibut stock increased significantly from a heavily depleted state in the early-1990s (Figure 10). The 81 cm size limit regulation enacted in 1994 caused a considerable reduction in legal-sized Atlantic Halibut biomass. Estimated spawning stock biomass in 2021 of 20.6 kt is approximately 42% of the equilibrium-unfished level of 48.36 kt. Total and legal Atlantic Halibut biomasses grew faster than the spawning stock because these state variables include either all ages (total biomass) or younger ages than currently appear in the female spawning stock (female maturity assumed 11.5 years at 50% and 14.5 years at 95%).

Model estimates of age-1 Atlantic Halibut abundance indicate two periods of high recruitment, one in the early 1970s and another recently from 2005–2014 (Figure 11). Recruitment estimates show alternating periods of above and below average recruitment, with better periods in the mid-1970s, late-1980s, and 2006–2014. The relationship between Atlantic Halibut spawning biomass and recruitment shows no consistent pattern with high and low recruitment occurring at both high and low spawning stock biomass levels (Figure 12). An increase in the recruitment process error allowed for the posterior distribution to correspond with an informative prior for moderate steepness and still gives the model the flexibility to produce high recruitment when spawning stock is low (Figure 13).

SISCAL model estimates of the legal-sized exploitation rates for each fleet suggest that current exploitation rates are near the long-term average of 0.145 (Figure 14). There was a short period of intense exploitation in the 1980s and early-1990s following the period of peak catches and stock decline. Notably the harvest rate has been fairly stable throughout the 2000s estimated to be just above U_{MSY}. In the last few years, the harvest rate has increased slightly from 0.107 in 2016 to 0.121 in 2021. The relationship between historical fishing mortality rates and spawning stock biomass suggest that fishing intensity increased during a period of low abundance, while fishing mortality over the past several years has been relatively stable and the recent period of high recruitment has resulted in spawning biomass that is twice SB_{MSY} (Figure 15). Equilibrium yield estimates are similar for harvest rates from 0.05 to 0.12, with U_{MSY} estimated to be 0.09 (Figure 16).

A comparison with SCAL show that SISCAL estimates higher levels of spawning biomass, while the pattern of recruitment is similar (Figure 17). There was some indication of a retrospective pattern for model estimates of spawning stock biomass where biomass increased more sharply with less data during the recent period of high recruitment and stock growth (Figure 18).

HARVEST STRATEGY SIMULATION RESULTS

All tested procedures with a ramped harvest control rule meet the first 2 conservation objectives (Table 10). There are no replicates or time-steps where Atlantic Halibut spawning biomass drops below the LRP of 0.4 B_{MSY} under a precautionary harvest control rule, meeting Objective 1 at both high and very high probabilities. In contrast, there is a 43% chance of dropping below the LRP under the current management procedure (conF_0.14_15%), which does not meet Objective 1 under any probability threshold. For Objective 2, while there is a very high probability of decline under all procedures, the current stock status above B_{MSY} means that any probability of decline is acceptable. Indeed, simulated population dynamics under all procedures show a decline towards B_{MSY} over the course of the simulations for all MPs except the No Fishing procedure (Figures 23–26).

Alternative harvest strategies are separated largely by their catch performance. As expected, there is a negative trade-off between catch variation (mAAC10, Table 10) and average yield (avgC, Table 10). There are higher average inter-annual changes in TAC under the fixed station survey than the stratified random survey (mAAC10, mAAC_2gen), ranging from 250 t to 330 t under the fixed survey, and between 160 t and 220 t under the random survey over the first 10 years. Catch variation patterns are similar over 2 generations, but with a slightly shorter range within each survey. The lower variation under the random survey shows that higher survey precision offsets the elevated uncertainty in catchability due to shorter random survey time series length. There is also a negative relationship between the short-term catches, which range between 3.5 kt and 4 kt (Table 10, avgC), and the number of years that TACs remain above 1.2MSY (Table 10, nPeak), which ranges from 10 to 13 years. Procedures with higher catches, such as the artic1.2Fmsy HCR and under the random survey, tend to have a shorter period of peak resource utilisation by about 1–2 years. The shortest period of peak resource utilisation is 10 years, under the rel170 procedures, indicating that the increased discard induced mortality under that management procedure leads to a net conservation loss, reducing survey biomass and lowering TACs in a shorter period, on average, than all other MPs.

By design, the artic1.2Fmsy HCR exerts higher fishing pressure on the stock, with higher probabilities of overfishing (Table 11, pOverfish), and a slightly higher mean over-fishing rate (Table 11, mU_Overfish). As a result, legal-sized harvest rates under the artic1.2Fmsy HCR tend to start out higher in 2022 (Figures 25 and 26), increase for several years under the fixed station survey (Figure 25), and gradually reduce towards the optimal legal harvest rate U_{MSY} = 0.087 over the projection as median biomass reaches or drops below B_{MSY} (Figures 25

and 26). Given the higher harvest rates, median Atlantic Halibut spawning biomass reaches B_{MSY} around 10 years earlier under the artic1.2Fmsy HCR than the rampedFmsy HCR, and in fact drops below B_{MSY} towards the upper stock reference when using the fixed station survey data, reflecting the lower precision of that survey. In contrast, the random survey does better at keeping biomass at or above B_{MSY} than the fixed station survey, and does the best when combined with the artic1.2Fmsy harvest control (articFmsy, HSrand plot).

The main differences between the release factors (higher minimum size limit and release of 170+ cm fish) were in the fishing pressure exerted on the stock. Since the TACs were all taken in full, and the “exploitable” portion of the biomass is reduced by shifting the minimum length higher, and there is higher discard mortality on large fish, so harvest rates on the legal-sized biomass increase (Table 11). As a result, peak resource utilisation comes to an end earlier than without the changes to size-based discarding (Tables 11). Given the base fecundity assumption, there are no conservation benefits to offset the changes in fishing pressure (See appendix B where we explore alternative fecundity scenarios).

Average yield over the first 10 years groups into two clusters based on the harvest control rule. Average catch (avgC, Table 10) under the artic1.2Fmsy HCR range between 3.9 and 4 kt, around 400–500 t more than average catches from the rampedFmsy HCR, which range between 3.4 and 3.5 kt. In the short-term, procedures using the fixed station survey and rampedFmsy HCR have lower TACs (Table 11, Figure 23) for 2022–2024 than procedures using either the random survey (Figures 24 and 26) of artic1.2Fmsy HCR (Figures 25 and 26), which reflects the large drop in the fixed station survey index in 2021, leading to a lower three-year average for the 2022–2024 period, as well as the lower target harvest rate with no change minimum under the rampedFmsy. However, after 2024, the median TACs under the fixed station survey correct back to a roughly linear trend from 2021 TACs down to around MSY at the end of the projection period.

DISCUSSION

The Scotian Shelf and southern Grand Banks Atlantic Halibut stock has a history of overfishing that pre-dates the time series used in the stock assessment model (i.e., prior to 1970). The new statistical catch-at-length assessment model (SISCAL) estimates historical biomass, fishing mortality, recruitment, and time-varying natural mortality. The 2021 spawning stock biomass estimate was 31.1 kt, with 95% credible interval (25, 36), the highest recorded estimate to date; total and legal-sized (greater than 81 cm) biomass are also at record levels. Current exploitation rates have remained reasonably constant, providing evidence that the constant F harvest strategy was achieved. Over the time series the estimated natural mortality, M, has varied. Recent (2014–2021) estimates of M ranging from 0.119 to 0.137, for males and from 0.111 to 0.128 for females. This stock has benefited from a recent period of high recruitment and has continued to increase from a depleted state observed in the 1990s.

In this paper, we fit a spatially-integrated statistical-catch-at-length (SISCAL) model, which is structurally similar to the SCAL model that was used in the last assessment. In its current implementation, the biggest change from SCAL to SISCAL is the inclusion of time-varying M. We have also updated the data for the assessment model with seven years of new data (Li et al. In press), including a new growth model with fit to increased age sample. A comparison of SISCAL to SCAL shows agreement in general biomass and recruitment trends, but differences in scale, which is standard between different models fit to the same data. Since the last assessment, Atlantic Halibut abundance indices and catches have both increased. Not surprisingly, these additional data results in adjustments to the scale of the model, creating a retrospective pattern in recent years (Figure 18). Both spawning stock biomass and recruitment

follow the same trends, but SISCAL estimates of SSB and recruitment are higher. Notably, for the 2014 SCAL model, interim reference points were used but the new SISCAL model provides reference points based on an equilibrium analysis of maximum sustainable yield (e.g., B_{MSY}).

As has been noted during previous assessments, the stock-recruitment relationship for Atlantic Halibut is difficult to describe with typical stock-recruitment models (Trzcinski and Bowen 2016, Cox et al. 2016). When the process error on recruitment was increased with SISCAL, an informative prior around h = 0.7, returns a posterior mean steepness of h = 0.73. The time-varying M estimates are all within the range predicted from meta-analysis and tagging (Li et al. In press, den Heyer et al. 2013), and SISCAL does estimate higher natural mortality during the early 1990s when a recruitment pulse produced higher catches in the DFO RV survey that did not result in a major increase in legal biomass. The spike in natural mortality in the early 1990s could be associated with unreported catch or high discard mortality during a period of intense fishing (Trzcinski and Bowen 2016).

In 2014, SCAL was used to condition an operating model and evaluate harvest control rules in closed-loop simulations. From those evaluations, a harvest control rule based on the Industry-DFO Halibut Longline Survey and DFO 4VWX Research Vessel survey index of recruitment was adopted. The adopted F = 0.14 management procedure (i.e., a constant target fishing mortality rate of 0.14) produced TAC advice by applying the target F to the q-adjusted 3-year mean of the Industry-DFO Halibut Longline Survey index of exploitable biomass. The F = 0.14 procedure was effective, with harvest rate estimates from SISCAL remaining reasonably constant ranging from 0.104 to 0.125 from 2014 to 2020, and recent 2021 estimates being (F = 0.12). Not surprisingly, because of the difference in scale between SISCAL and SCAL the F estimate from SISCAL is lower than the target F = 0.14.

Here, we used SISCAL-AH to condition an updated operating model and tested new candidate management procedures for Atlantic Halibut using closed-loop simulations against Atlantic Halibut fishery management objectives. The previous interim management procedure (MP), a constant F rule, was tested, alongside 16 MPs based on new DFO precautionary approach compliant harvest control rules, the survey data used to estimate stock status, and 4 combinations of size-based discarding options. Closed-loop simulation results showed two main outcomes. First, the current catch levels can likely be gradually reduced to MSY levels over 12–14 years with low conservation risk. Both tested harvest control rules kept catches higher than 120% of estimated MSY, despite lower reference removal rates. Second, increased precision of the random survey design offsets higher uncertainty in catchability due to the shorter time series of observations. Therefore, there may be a yield benefit from switching to the random survey sooner rather than later, avoiding a short-term drop in TACs from the very low 2021 fixed station survey index, while the 2021 random survey index was proportionally much higher.

Articulated harvest control rules that allow for a small amount of overfishing in the healthy zone show promise but could benefit from additional tuning to meet Fish Stocks Provisions requirements. While articulated HCRs did not violate either of the Atlantic Halibut conservation objectives, the higher short-term yields do reduce the period of peak resource utilisation by around 2–3 years. Furthermore, higher fishing pressure brings biomass down to the target B_{MSY} much faster than the ramped HCR, and sometimes overshoots the target when using the less precise fixed station survey, producing higher effective harvest rates.

Uncertainty in abundance indices, fisheries data, and biological data (for review see: Shackell et al. 2021, Li et al. In press) may lead to biased estimates from the assessment model. There remain questions about the fisheries data, which could be explored through simulations such as the functional form of size-selectivity by the longline fishery. As larger Atlantic Halibut are

primarily mature females, reproductive behaviours and/or changes in distribution may affect fishery and/or survey catchability. Additionally, given the reduced commercial value of large Atlantic Halibut, there may be modifications in fishing practices aimed at reducing catch of large Atlantic Halibut. A new growth model based on samples up until 2018 has been used in the assessment. While it is known that there is spatial variation in growth (Shackell et al. 2019, Zheng et al. In prep.[1]), this simplified model used here does not address the spatial and temporal variation. Spatial and temporal variability in other biological parameters, such as maturity-at-age and fecundity, may also introduce uncertainties in the SISCAL model.

There is potential for considerable variability in biology of this Atlantic Halibut stock across the large management unit area (for review see: Shackell et al. 2021). The current implementation SISCAL, like SCAL, has a fleets-as-areas approach to better describe the removals, for which there is evidence, such as spatial variation in the length composition data, but SISCAL is not limited to this approach. For example, spatial differences in growth/weight-at-age could be used when removing catch from the population, or SISCAL could be expanded to a spatially explicit model, as the specification includes nascent functionality for spatially explicit sub-areas that are linked by age-dependent movement.

Additionally, it has been increasingly recognized that environmental factors have significant impacts on recruitment, growth, and reproduction. With warmer temperatures, many fish species grow faster and demonstrate smaller size-at-age and younger maturity-at-age. There is a growing literature linking changes in Atlantic Halibut distribution and abundance to changes in the thermal regime (Shackell et al. 2021, Li et al. In press, Czich et al. submitted). However, lacking a clear mechanism between the physical factors and biological processes, we are unable to incorporate these into the SISCAL.

The Scotian Shelf and southern Grand Banks Atlantic Halibut stock is on a multi-year assessment cycle, with harvest advice provided in interim years based on a predetermined procedure, and it has been seven years since the last assessment. The updated SISCAL model described here will provide a basis for updating the MSE approach for establishing new harvest strategies and interim assessment procedures.

REFERENCES CITED

Armsworthy, S.A., and Campana, S.E. 2010. Age determination, bomb-radiocarbon validation and growth of Atlantic halibut (*Hippoglossus hippoglossus*) from the Northwest Atlantic. Environ. Biol. Fish. 89: 279-295.

Bowering, W.R. 1986. The distribution, age and growth and sexual maturity of Atlantic halibut (*Hippoglossus hippoglossus*) in the Newfoundland and Labrador area of the Northwest Atlantic. Can. Tech. Rep. Fish. Aquat. Sci. 1432: 34p.

Cox S.P., A. Benson, and C.E. den Heyer. 2016. Framework for the Assessment of Atlantic Halibut Stocks on the Scotian Shelf and Southern Grand Banks. DFO Can. Sci. Advis. Sec. Res. Doc. 2016/001. v + 57 p.

den Heyer, C.E., C.J. Schwarz, and M.K. Trzcinski. 2013. Fishing and Natural Mortality Rates of Atlantic Halibut Estimated from Multiyear Tagging and Life History. Transactions of the American Fisheries Society 142: 690–702.

Francis, R. C. (2014). Replacing the multinomial in stock assessment models: A first step. Fisheries Research, 151: 70–84.

Kristensen, K., Nielsen, A., Berg, C. W., Skaug, H., and Bell, B. (2015). TMB: Automatic differentiation and Laplace approximation. arXiv preprint arXiv:1509.00660.

Li, L., Hubley, B., Harper, D.L., Wilson, G., and den Heyer, C.E. In press. Data Review and Assessment Model Update: Assessment of Atlantic Halibut on the Scotian Shelf and Southern Grand Banks (NAFO Divs. 3NOPs4VWX5Zc) Data Inputs and Model. DFO Can. Sci. Advis. Sec. Res. Doc.

McCracken, F.D. 1958. On the biology and fishery of the Canadian Atlantic halibut *Hippoglossus hippoglossus* L. J. Fish. Res. Bd. Canada. 15(6): 1269-1311.

Monnahan, C. C. and Kristensen, K. (2018). No-u-turn sampling for fast Bayesian inference in ADMB and TMB: Introducing the adnuts and tmbstan r packages. PloS one, 13(5):e0197954.

Monnahan, C. C., Thorson, J. T., and Branch, T. A. (2017). Faster estimation of Bayesian models in ecology using Hamiltonian Monte Carlo. Methods in Ecology and Evolution, 8(3): 339–348.

Neilson, J.D. and Bowering W.R. 1989. Minimum size regulations and the implications for yield and value in the Canadian Atlantic halibut fishery. Can. Atl. Fisheries Sci. Adv. Comm. 89/5.

Perley, P., Neilson, J.D., and Zwanenberg, K. 1985. A review of the status of the 4VWX halibut stocks. Can. Atl. Fish. Sci. Advisory Comm. Res. Doc. 85/43 23p.

R Core Team (2015). R: A Language and Environment for Statistical Computing. R Foundation for Statistical Computing, Vienna, Austria.

Schnute, J. T. and Haigh, R. (2007). Compositional analysis of catch curve data, with an application to *Sebastes maliger*. ICES Journal of Marine Science: Journal du Conseil, 64(2):218–233.Boudreau, S.A., N.L. Shackell, S. Carson, and C.E. den Heyer. 2017. Connectivity, persistence, and loss of high abundance areas of a recovering marine fish population in the Northwest Atlantic Ocean. Ecol. Evol. 7(22): 9739–9749. doi:10.1002/ece3.3495.

Shackell, N.L., K.J. Ferguson, C.E. den Heyer, D. Brickman, Z. Wang and K.T. Ransier. 2019. Growing degree-day influences growth rate and length of maturity of Northwest Atlantic halibut (*Hippoglossus hippoglussus* L.) across the southern stock domain. Journal of Northwest Atlantic Fishery Science. 50: 25–35. doi:10.2960/J.v50.m716

Shackell N.L., J.A.D. Fisher, C.E. den Heyer, D.R. Hennen, A.C. Seitz, A. Le Bris, D. Robert, M.E. Kersula, S.X. Cadrin, R.S. McBride, C.H. McGuire, T. Kess, K.T. Ransier, C. Liu, A. Czich and K.T. Frank. 2021. Spatial Ecology of Atlantic Halibut across the Northwest Atlantic: A Recovering Species in an Era of Climate Change. Rev. Fish. Sci. Aquacul. DOI: 10.1080/23308249.2021.1948502

Stewart, I., and A. Hicks. 2019. 2019 Pacific halibut (*Hippoglossus stenolepis*) stock assessment: Development. IPHC-2019-SRB014-07:1-100.

Stobo, W., Neilson, J.D., and Simpson, P. 1988. Movements of Atlantic halibut (*Hippoglossus hippoglossus*) in the Canadian North Atlantic: inference regarding life history. Can. J. Fish. Aquat. Sci. 45: 484-491.

Trzcinski, M.K. and Bowen, W.D. 2016. The recovery of Atlantic halibut: a large, long-lived, and exploited marine predator. ICES Journal of Marine Science 73(4): 1104–1114. doi: 10.1093/icesjms/fsv266.

Trzcinski, M.K., Armsworthy, S.L., Wilson, S., Mohn, R.K., and Campana, S.E. 2011. A framework for the assessment of the Scotian Shelf and Southern Grand Banks Atlantic halibut stock. DFO Can. Sci. Advis. Sec. Res. Doc. 2011/02.

Zwanenburg, K.C.T., Black, G., Fanning, P., Branton, R., Showell, M., and Wilson, S. 1997. Atlantic halibut (*Hippoglossus hippoglossus*) on the Scotian Shelf and Southern Grand Banks: evaluation of resource status. DFO Can. Sci. Advis. Sec. Res. Doc. 1997/050. 75 p.

TABLES

Table 1. Total landings data for longline in Area 3 (LL3) and Area 4 (LL4) and otter trawl in Area 3 (OT3) and Area 4 (OT4).

Year	LL3	LL4	OT3	OT4
1970	249	603	440	270
1971	319	676	244	399
1972	172	716	319	154
1973	206	722	287	117
1974	147	600	287	78
1975	150	563	255	145
1976	107	567	238	175
1977	89	503	500	188
1978	73	709	256	306
1979	52	856	365	329
1980	71	1050	218	443
1981	61	1100	172	359
1982	74	1414	417	383
1983	136	1597	137	312
1984	600	1826	323	204
1985	906	1772	951	231
1986	904	1467	752	140
1987	582	1070	799	103
1988	763	1216	259	131
1989	600	1136	164	70
1990	603	1017	487	132
1991	278	802	801	138
1992	284	875	166	105
1993	252	758	112	140
1994	127	856	97	36
1995	139	520	86	47
1996	118	581	51	37
1997	152	692	75	34
1998	201	564	90	18
1999	186	585	148	27
2000	254	509	92	7
2001	394	722	159	44
2002	348	721	199	53
2003	442	779	312	50
2004	349	800	129	82
2005	334	766	69	65
2006	339	872	35	50
2007	489	899	37	88
2008	363	960	53	59
2009	297	1180	510	73
2010	421	1241	118	67
2011	419	1265	133	94
2012	539	1377	139	131
2013	520	1757	213	99
2014	756	1729	314	106
2015	613	2093	414	107
2016	366	2116	634	110

Year	LL3	LL4	OT3	OT4
2017	649	2251	490	127
2018	585	2993	452	191
2019	727	3184	586	202
2020	1196	3458	398	198

Table 2. Notation used in the SISCAL model. A dash (-) indicates not applicable.

Symbol	Value	Description
T	44	Total number of time steps 1951–2019
A	30	Plus group age-class
l	7.5,12.5, …,262.5	Length bin midpoints ($L = 52$ length bins in total)
t	$1,2,\ldots,T$	Time step
a	$1,2,\ldots,A$	Age-class index
g	$1,2,\ldots,7$	Gear index for (1) LL_NAFO3, (2) LL_NAFO4, and (3) OT_NAFO3, (4) OT_NAFO4, (5) RV_4VWX, (6) HS_Fixed, (7) HS_Random
x	1,2	Sex index for male (1) and female (2) fish for model states, and in length compositions collected at sea, (3) combined sexes
m_a	-	Maturity-at-age a
$a_{50}^{mat}, a_{95}^{mat}$	11.5, 14.5	Age-at-50% and age-at-95% maturity
B_0	-	Unfished female spawning stock biomass
h	-	Beverton-Holt stock-recruitment steepness
R_0	-	Unfished equilibrium recruitment
$\underline{R}$	-	Average recruitment
R_{init}	-	1970 recruitment for fished initialisation
$S_{a,x}$	-	Unfished equilibrium survivorship-at-age-a for sex x
$w_{a,x}$ a b	 0.00673 3.12	Weight-at-age a for sex x Length-Weight relationship a Length-weight relationship b
l_0	0.685	Theoretical length-at-age 0 (both sexes)
$L_{\infty,x}$	120.81,200.22	Asymptotic mean length for sex x (cm)
K_x	0.08,0.04	Von Bertalanffy growth coefficient for sex x
λ_x	1.35,1.33	
$l_{a,x}$	-	Mean length-at-age-a for sex x
$\sigma_{L,x}$	0.18,0.12	CV in length-at-age distribution for males and females
c_1, c_2	-	Allometric length-weight conversion parameters
ϕ_0	-	Unfished equilibrium spawning biomass per recruit
α_h, β_h	56.82,21.02	Beta prior parameters for steepness
ω_t	-	Annual recruitment process error log-deviations
σ_R	0.75	Standard error of ω_t recruitment deviations
q_g	-	Catchability coefficient for RV_4VWX ($g = 5$), HS_Fixed ($g = 6$), and HS_Random ($g = 7$) surveys
$M_{x,t}$	-	Annual natural mortality rates for male and female fish
$s_g^{50,A}$	-	Length-at-50% selectivity for gear g (Ascending limb)
$s_g^{Step,A}$	-	Difference between length-at-50% and length-at-95% selectivity for gear g (Ascending limb)
$s_g^{Step,1,D}$	-	Difference between length-at-95% ascending and length-at-95% descending selectivity for gear g (g = 3, 4, 5)
$s_g^{Step,2,D}$	-	Difference between length-at-50% and length-at-95% selectivity for gear g (Descending limb, g = 3, 4, 5)
δ_g	-	Fractional time-step at which catch from gear type g is removed from the population
$L_{lim,g,t}$	81	Minimum size limit applied to commercial landings for gear g in year $t \geq t_g^{lim}$

Symbol	Value	Description
t_g^{lim}	1988, 1988, 1990, 1995	First year of discarding fish below the legal size
d_g	0.23,1.26	Instantaneous discard induced mortality rate (resp, longline and trawl)
$p_{a,x,g}^{Rel}$	-	Probability of releasing an age a fish of sex x when caught by gear g (post first year of size limit)
$N_{a,x,t+\delta_g}$	-	Total numbers-at-age a for sex x in year t at fractional time-step δ_g
$N_{a,x,g,t+\delta_g}$	-	Total numbers-at-age a for sex x vulnerable to gear g in year t at fractional time-step δ_g
$B_{p,t}$	-	Spawning biomass of area p in year t
$C_{g,t}$	-	Observed landings from gear g at time t (kilotonnes)
$\hat{C}_{g,t}$	-	Estimated total catch (landings and releases) from gear g at time t (kilotonnes)
$\widehat{D}_{g,t}$	-	Estimated total discards (releases) from gear g at time t (kilotonnes)
$C_{a,x,g,t}$	-	Expected catch-at-age a in numbers from sex x by gear g in year t
$C'_{a,x,g,t}$	-	Expected catch-at-age a in biomass units from sex x by gear g in year t
$U_{g,t}$	-	Harvest rate by gear g in year t
$I_{g,t}$	-	Observed survey index for gear $g \in \{5,6\}$ at time t
$\hat{I}_{g,t}$	-	Expected survey index for gear $g \in \{5,6\}$ at time t
τ_g	-	Standard deviation of survey index observation log-residuals
$u_{l,x,g,t}$	-	Observed composition data for length bin l from gear g at time t
$\hat{u}_{l,x,g,t}$	-	Expected composition data for length bin l from gear g at time t
$B_{x,g,t}$	-	Total number of length bins with age observations above 2% of the total sample size in year t
$\tau_{p,g}^{len}$	-	Conditional MLE of age composition sampling error
ρ_g	-	Correlation-at-lag-1 coefficient for length composition residuals
C	-	Lag-1 correlation matrix for length composition residuals
K	-	Dimension transformation matrix for length composition logistic normal likelihood
$\iota_{x,g,t}$	-	Centred logistic normal length-composition log-residuals for sex x in gear g at time step t
$p_{l,g,t}^F$	-	Proportion of observations in length bin l that were female
$\hat{p}_{l,g,t}^F$	-	Expected Proportion of fish in length bin l that are female
$p_{alloc,g}$	0.2507, 0.6899, 0.0258, 0.0337	Proportion of TAC allocated to each fleet (g = 1, …, 4)

Table 3. Process model equations for the SISCAL model.

No.	Equation
(P.1)	$\Theta^{lead} = \left(B_0, \underline{R}, \{\omega_t\}_{t\in 1:T}, M_{x,1}, \{\epsilon_t\}_{t=2:T}, s_g^{(50)}, s_g^{(step)}, s_g^{Step,1,D}, s_g^{Step,2,D}\right)$
(P.2)	$\Theta^{cond} = \left(\{logq_g\}_{g\in 5,6}, \{\tau_g\}_{g\in 5,6}, \{\tau_g^{age}\}_{g\in 1:6}, \{\tau_g^{p^F}\}_{g\in 1:6}\right)$
(P.3)	$\Theta^{fixed} = (\{m_a\}_{a\in 1:30}, \sigma_R, \sigma_M)$
(P.4)	$\Theta^{priors} = \left(m_M, s_M, \{m_g^{s^{50,A}}, m_g^{s^{Step,A}}, m_g^{s^{Step,1,D}}, m_g^{s^{Step,2,D}}, \sigma_g^{Sel}\}_{g\in 1:3}, \alpha_h, \beta_h\right)$
(EQ.1)	$m_a = \left(1 + e^{-log19\frac{a-a_{50}^{mat}}{a_{95}^{mat}-a_{50}^{mat}}}\right)^{-1}$
(EQ.2)	$M_{x,t} = \{M_{x,1}\ t\ =\ 1, M_{x,t-1}\cdot e^{\epsilon_t}\ t\ \geq\ 2.$
(EQ.3)	$M_{0,x} = \frac{1}{T}\sum_t\ M_{x,t}$
(EQ.4)	$S_{a,x} = \{0.5\ a = 1, S_{a-1,x}e^{-M_{0,x}}\ 1 < a < A\ S'_{a-1,x}e^{-M_{0,x}}/(1-e^{-M_{0,x}})\ a = A.$
(EQ.5)	$\phi_0 = e^{-M_{0,x=1}}\cdot\sum_a\ S_{a,x=1}\cdot w_{a.x=1}\cdot m_a$
(EQ.6)	$R_0 = \frac{B_0}{\phi_0}$
(EQ.7)	$N_{a,x}^{eq} = R_0\cdot S_{a,x}$
(G.1)	$l_{a,x} = L_{\infty,x}\cdot\left[1-\left(1-\frac{l_0}{L_{\infty,x}}\right)e^{-K_x a^{\lambda_x}}\right]$
(G.2)	$D(a,x) = e^{-\frac{(l-l_{a,x})^2}{2(\sigma_L\cdot l_{a,x})^2}}$
(G.3)	$P(a,x) = \frac{D(a,x)}{\sum_{l'}\ D(a,x)}$
(S.1)	$s_{a,x,g} = \{\frac{\left(1+e^{-log19\frac{l_{a,x}-s_g^{50,A}}{s_g^{Step,A}}}\right)^{-1}}{S_{a\prime,x,g}}\ g\ =\ 1,2,6,7\ \frac{\left(1+e^{-log19\frac{l_{a,x}-s_g^{50,A}}{s_g^{Step,A}}}\right)^{-1}\left(1+e^{-log19\frac{l_{a,x}-s_g^{50,D}}{s_g^{Step,D}}}\right)^{-1}}{S_{a\prime,x,g}}\ g$ $=\ 3,4,5$
(NEQ.1)	$N_{a,x,1} = R_{init}\cdot S_{a,x}$
(D.1)	$p_{a,x,g}^{Rel} = \sum_l\ 1\left(l_{a,x} < l_g^{lim}\right)\cdot P(a,x)$
(C.1)	$N_{a,x,t+\delta_g} = N_{a,x,t+\delta_{g-1}}\cdot e^{-1\cdot(\delta_g-\delta_{g-1})M_{x,t}}$
(C.2)	$N_{a,x,g,t} = N_{a,x,t+\delta_g}\cdot s_{a,x,g}$
(C.3)	$B_{a,x,g,t} = N_{a,x,g,t}\cdot w_{a,x}$
(C.4)	$B_{g,t} = \sum_{a,x}\ B_{a,x,g,t}$
(C.5)	$p_{a,x,g,t}^{(B)} = \frac{B_{a,x,g,t}}{B_{g,t}}$
(C.6)	$\widehat{C_{g,t}} = \frac{C_{g,t}}{\sum_{a,x}\ \left[\left(1-p_{a,x,g}^{Rel}\right)\cdot p_{a,x,g,t}^{(B)}\right]}$

No.	Equation
(C.7)	$C'_{a,x,g,t} = \widehat{C_{g,t}} \cdot \frac{B_{a,x,g,t}}{B_{g,t}}$
(C.7)	$C_{a,x,g,t} = \frac{C'_{a,x,g,t}}{w_{a,x,g,t}}$
(C.8)	$D_{a,x,g,t} = C_{a,x,g,t} \cdot p^{Rel}_{a,x,g}$
(C.9)	$N_{a,x,t+\delta_g^+} = N_{a,x,t+\delta_g} - C_{a,x,g,t} + D_{a,x,g,t} e^{-d_g}$
(C.10)	$U_{g,t} = \frac{C_{g,t}}{B_{g,t}}$
(A.1)	$B_t = \sum_a N_{a,x=1,t} \cdot w_{a,x=1,t} \cdot m_a$
(A.2)	$R_{t+1} = \underline{R} \cdot e^{\omega_t}$
(A.3)	$\hat{R}_{t+1} = \frac{4hR_0B_t}{(B_0(1-h)(1-(5h-1)/(B_0(1-h))B_t)}$
(A.3)	$N_{a,x,t+1} = \{0.5\ R_{t+1}\ a = 1\ e^{-(1-\delta_G)M_{x,t}} \cdot N_{a-1,x,t+\delta_G}\ 2 \le a \le A-1\ e^{-(1-\delta_G)M_{x,t}} \cdot (N_{a-1,x,t+\delta_G} + N_{a,x,t+\delta_G})\ a = A.$

Table 4. Data likelihoods, model prior density functions, and the final objective function for the SISCAL. $1(X)$ is the indicator function that takes value 1 when the statement X is true, and 0 otherwise.

No.	Equation
(O.1)	$X_{g,t} = \{N_{g,t}\ g = 5\ B_{g,t}\ g = 6,7$
(O.2)	$\hat{u}_{l,x,g,t} = \{0\ l < L_{lim,g,t}\ and\ t \ge t^{lim}_{g,t} \sum_a \frac{P(a,x)N_{\{a,x,g,t\}}}{\sum_{\{l'\}} P(a,x)N_{\{a,x,g,t\}}}\ l > L_{lim,g,t}\ OR\ t < t^{lim}_{g,t}$
(O.3)	$\hat{p}^F_{l,g,t} = \{0\ l < L_{lim,g,t}\ and\ t \ge t^{lim}_{g,t} \frac{\sum_a P(a,x=2)N_{a,x=2,g,t}}{\sum_a P(a,x=1)N_{a,x=1,g,t} + \sum_a P(a,x=2)N_{a,x=2,g,t}}\ l > L_{lim,g,t}\ OR\ t < t^{lim}_{g,t}$
(NLL.1)	$z_{g,t} = \{0\ I_{g,t} = 0\ log \frac{I_{g,t}}{X_{g,t}}\ I_{g,t} > 0$
(NLL.2)	$n_g = \sum_{t=1}^{T} 1(I_{g,t} > 0)$
(NLL.3)	$\widehat{q_g} = \frac{1}{n_g} \sum_t z_{g,t}$
(NLL.4)	$\hat{\tau}^2_g = \frac{1}{n_g} \sum_{t=1}^{T} 1(I_{g,t} > 0) \cdot (z_{g,t} - \widehat{q_g})^2$
(NLL.5)	$l_{g,1} = \frac{1}{2}(n_g \cdot log\ log\ \hat{\tau}^2_g + n_g)$
(L.1)	$C_g = [\rho_g^{j-i}]_{i,j}$
(L.2)	$K = [I_{L-1}\|1]$
(L.3)	$V_g = K \cdot C_g \cdot K^T$
(L.4)	$W_{p,g,t} = \frac{mean(n^{Len}_{x,g,t})}{n^{Len}_{x,g,t}}$
(L.5)	$B_{x,g,t} = \sum_l 1(u_{l,x,g,t} > 0.02)$
(L.6)	$\vec{l}_{x,g,t} = \langle log\ (u_{l,x,g,t}/u_{B_{x,g,t},x,g,t}) - log\ (\hat{u}_{l,x,g,t}/\hat{u}_{B_{x,g,t},x,g,t} \rangle_l$

No.	Equation
(L.7)	$$\hat{\tau}_{x,g}^{len} = \left(\frac{\sum_t \quad \frac{1}{W_{x,g,t}^2} (\vec{\imath}_{x,g,t})^T \cdot V_g^{-1} \cdot \vec{\imath}_{x,g,t}}{\sum_t \quad B_{x,g,t}} \right)^{0.5}$$
(L.8)	$$l_2 = \sum_{x,g} \quad \left(\sum_{l,t} \quad log u_{l,x,g,t} + log \hat{\tau}_{x,g}^{len} \sum_t \quad (B_{x,g,t} - 1) + \frac{1}{2} \sum_t \quad log \lvert V_g \rvert + \sum_t \quad (B_{x,g,t} - 1) log W_{x,g,t} \right)$$
(F.1)	$$n_g^{p^F} = \sum_{t,l} \quad 1\left(p_{g,t,l}^F > 0\right)$$
(F.2)	$$z_{l,g,t}^{p^F} = \{0 \; p_{g,t,l}^F = 0 \; or \; \hat{p}_{g,t,l}^F = 0 \; log\left(p_{g,t,l}^F\right) - log\left(\hat{p}_{g,t,l}^F\right) \; p_{g,t,l}^F > 0 \; and \; \hat{p}_{g,t,l}^F > 0$$
(F.3)	$$\hat{\tau}_g^{p^F} = \left(\frac{1}{n_g^{p^F}} \sum_{l,t} \quad \left(z_{l,g,t}^{p^F} \right)^2 \right)^{0.5}$$
(F.4)	$$l_{g,3} = \frac{1}{2} \left(n_g^{p^F} \cdot log \; log \; \left(\hat{\tau}_g^{p^F} \right)^2 + n_g^{p^F} \right)$$
(P.1)	$$p_1 = \sum_t \quad \omega_t^2$$
(P.2)	$$p_4 = \frac{1}{2\sigma_M^2} \sum_t \quad \epsilon_t^2$$
(P.3)	$$p_2 = (1 - \alpha_h) \; log \; log \; h \; + (1 - \beta_h) \; log \; log \; (1 - h)$$
(P.4)	$$p_3 = \sum_{g=1}^{4} \quad \left(log \; F_{init,g} \right)^2$$
(P.5)	$$p_5 = \sum_x \quad \left[\frac{\left(log \; log \; M_{0,x} \; - log \; log \; m_M \right)^2}{2s_M^2} + \frac{\left(log \; log \; \underline{M_x} \; - log \; log \; m_M \right)^2}{2s_M^2} \right]$$
(P.6)	$$p_6 = log \; log \; B_0 \; + log \; log \; \underline{R} \; + log \; log \; R_{init}$$
(P.7)	$$p_7 = \frac{1}{2\sigma_R^2} \sum_t \quad \left(log \; log \; R_t \; - log \; log \; \widehat{R_t} \right)^2$$
(F.1)	$$f = \sum_g \quad l_{g,1} + l_2 + \sum_g \quad l_{g,3} + p_1 + p_2 + p_3 + p_4 + p_5 + p_6 + p_7$$

Table 5. Atlantic Halibut fishery management objectives.

No	General intent	Aspirational objective	Measure	Probability	Time
1	Avoid low abundance where recruitment could be impaired (DFO)	Avoid fishery-induced decline of spawning biomass below LRP	Spawning biomass (SSB) below LRP	Low to Very-low	2 gen
2	Adjust level of precaution depending on stock status (DFO SFF Table 1)	Promote growth or mitigate decline when spawning biomass is between the LRP and USR	Spawning biomass status and trend	Probability of decline Low to Very Low at LRP to Neutral at USR	1 gen
3	Provide stable inter-annual TACs (Industry)	Avoid large inter-annual changes in TAC	Absolute (up or down) annual change in TAC	NA	2022–2031
4	Provide stable inter-annual TACs (Industry)	Avoid minor inter-annual changes in TAC	Absolute (up or down) annual change in TAC	NA	2022–2031
5	Optimize yield while avoiding boom-bust cycle	a.) Maximize yield b.) Extend duration of peak resource utilization c.) Avoid large intra-period changes in TAC	Yield Years Absolute TAC change	Neutral Neutral Neutral	2022–2031 2022–2031 2 gen

Table 6. Atlantic Halibut fishery management performance metrics. Numbers (No. column) correspond to fishery management objectives in Table 5. The function $1(X)$ is the indicator function, which takes value 1 when X is true, and 0 otherwise. A dash (-) indicates not applicable.

No.	Metric Name	Definition	Target
1	pLRP	$P(B < LRP) = \frac{\sum_t \sum_i 1(B_{i,t} < LRP)}{28 \cdot 100}$	Low: 5% to 25% Very low: 5%
2	pDecline	$P(B_{2035} < B_{2021}) = \frac{\sum_i 1(B_{i,2035} < B_{2021})}{100}$	Very low (5%) at LRP to Neutral (50%) at USR.
3, 4	mAAC10	$AAC_{10} = \frac{\sum_i \sum_{t=2022}^{2031} \lvert C_{i,t} - C_{i,t-1} \rvert}{10 \cdot 100}$	Minimise
5 a)	avgC	$\underline{C} = median_i \frac{\sum_t C_{i,t}}{28}$	Maximise
5 b)	nPeak	$\underline{N_{peak}} = median_i \left\{ max_{t>2021} \left[\sum_{t'=2022}^{t} 1(C_{i,t'} > 0.75\, C_{2021}) \right] \right\}$	Maximise
5 c)	mAAC28	$AAC_{28} = \frac{\sum_i \sum_{t=2022}^{2050} \lvert C_t - C_{t-1} \rvert}{28 \cdot 100}$	Minimise
-	pHealthy	$P(B > USR) = \frac{\sum_t \sum_i 1(B_{i,t} < 0.8\, B_{MSY})}{28 \cdot 100}$	-
-	pTarget	$P(B > TRP) = \frac{\sum_t \sum_i 1(B_{i,t} > B_{MSY})}{28 \cdot 100}$	-
-	p > U_{MSY}	$P(U > U_{MSY}) = \frac{\sum_t \sum_i 1(U_{i,t} > U_{MSY})}{28 \cdot 100}$	Neutral: 50%
-	mU_Overfish	$E(U \mid U > U_{MSY}) = \frac{\sum_t \sum_i U_{i,t} \cdot 1(U_{i,t} > U_{MSY})}{\sum_t \sum_i 1(U_{i,t} > U_{MSY})}$	-

Table 7. Management procedure (MP) factors and their levels used to define a grid of Atlantic Halibut MPs for evaluation in closed-loop simulations.

Factor	**Levels**	**Description**
Survey	HSfix	Fixed station Industry-DFO Halibut Longline Survey
	HSrand	Stratified random Industry-DFO Halibut Longline Survey
Harvest Control Rule	rampedFmsy	Ramped precautionary harvest control rule with 2 control points $F(LRP) = 0.05$ $F(USR) = F_{MSY}$
	Articulated1.2Fmsy	Precautionary harvest control rule with 3 control points: $F(LRP) = 0.05$ $F(USR) = 0.8F_{MSY}$ $F(1.2B_{MSY}) = 1.2F_{MSY}$
Size limit	sl81	81cm legal size limit
	sl86	86cm legal size limit
Voluntary release of large fish	rel170	80% release rate of 170+ cm Halibut
	keep170	No release of 170+ cm Halibut

Table 8. Maximum sustainable yield (MSY) based reference points for Atlantic Halibut spawning biomass, and fixed station and stratified random portions of the Industry-DFO Halibut Longline Survey biomass. Survey biomass reference points are derived from model equilibrium survey biomass at long-term fishing mortality rates that produce the female spawning biomass levels shown. A dash (-) indicates not applicable.

Biomass	**LRP**	**USR**	B_{MSY}	**Catchability** q
Female Spawning Biomass	5.3 kt	10.6	13.3 kt	-
Fixed station survey biomass	11.8 kt	23.52	29.4 kt	0.0046
Stratified random survey biomass	10.9 kt	21.84	27.3 kt	0.0020

Table 9. Mathematical definitions of the two precautionary harvest control rules tested in closed-loop simulations.

Rule	**Definition**	**Interannual limit on TAC changes**
rampedFmsy	$$F(\widehat{B_t}) = \begin{cases} 0.05 & if \quad \widehat{B_t} \le LRP \\ \frac{(\widehat{B_t} - LRP)(F_{MSY} - 0.05)}{(0.8B_{MSY} - LRP)} & if \quad LRP < \widehat{B_t} \le 0.8B_{MSY} \\ F_{MSY} & if \quad \widehat{B_t} > 0.8\,B_{MSY} \end{cases}$$	$$\Delta_t(\widehat{B_t}) = 1.0$$
artic1.2Fmsy	$$F(\widehat{B_t}) = \begin{cases} 0.05 & if \quad \widehat{B_t} \le LRP \\ 0.05 + \frac{(\widehat{B_t} - LRP)(0.8F_{MSY} - 0.05)}{(0.8B_{MSY} - LRP)} & if \quad LRP < \widehat{B_t} \le 0.8B_{MSY} \\ \left(0.8 + \frac{0.4(\widehat{B_t} - 0.8B_{MSY})}{(1.2B_{MSY} - 0.8B_{MSY})}\right)F_{MSY} & if \quad 0.8B_{MSY} < \widehat{B_t} \le 1.2B_{MSY} \\ 1.2F_{MSY} & if \quad \widehat{B_t} > 0.8\,B_{MSY} \end{cases}$$	$$\Delta_t(\widehat{B_t}) = \begin{cases} 1.0 & if \quad \widehat{B_t} \le LRP \\ 1 - \frac{(\widehat{B_t} - LRP)(1 - 0.15)}{(0.8B_{MSY} - LRP)} & if \quad LRP < \widehat{B_t} \le 0.8B_{MSY} \\ 0.15 & if \quad \widehat{B_t} > 0.8\,B_{MSY} \end{cases}$$

Table 10. Management performance metrics for the 18 tested Atlantic Halibut management procedures. Conservation metrics are measured in probability (proportion of simulations and time steps), and a bullet (·) indicates that the performance threshold for decline probability, based on the stock status in 2021, has been met. The catch metrics mAAC10, avgC, and mAAC_2gen are in kt units, and nPeak is in years are defined in Table 6.

MP	Max F	Min Size Limit	pLRP	pDecline	mAAC10	avgC	nPeak	mAAC_2gen
NoFish	0	81	0.00	0	0.00	0.00	0	0.00
conF.14_15%	0.14	81	0.44	·	0.47	5.50	13	0.33
HSfix_rampedFmsy_sl81_rel170	0.087	81	0.00	·	0.25	3.50	10	0.24
HSfix_artic1.2Fmsy_sl81_rel170	0.103	81	0.00	·	0.33	3.90	10	0.30
HSfix_rampedFmsy_sl86_rel170	0.087	86	0.00	·	0.25	3.40	10	0.24
HSfix_artic1.2Fmsy_sl86_rel170	0.103	86	0.00	·	0.33	3.90	10	0.30
HSfix_rampedFmsy_sl81_keep170	0.087	81	0.00	·	0.25	3.50	11	0.24
HSfix_artic1.2Fmsy_sl81_keep170	0.103	81	0.00	·	0.33	4.00	11	0.31
HSfix_rampedFmsy_sl86_keep170	0.087	86	0.00	·	0.25	3.50	12	0.24
HSfix_artic1.2Fmsy_sl86_keep170	0.103	86	0.00	·	0.33	4.00	11	0.31
HSrand_rampedFmsy_sl81_rel170	0.087	81	0.00	·	0.16	3.50	10	0.16
HSrand_artic1.2Fmsy_sl81_rel170	0.103	81	0.00	·	0.23	3.90	10	0.22
HSrand_rampedFmsy_sl86_rel170	0.087	86	0.00	·	0.16	3.50	10	0.16
HSrand_artic1.2Fmsy_sl86_rel170	0.103	86	0.00	·	0.23	3.90	10	0.22
HSrand_rampedFmsy_sl81_keep170	0.087	81	0.00	·	0.16	3.50	11	0.16
HSrand_artic1.2Fmsy_sl81_keep170	0.103	81	0.00	·	0.22	4.00	11	0.22
HSrand_rampedFmsy_sl86_keep170	0.087	86	0.00	·	0.16	3.50	12	0.16
HSrand_artic1.2Fmsy_sl86_keep170	0.103	86	0.00	·	0.22	4.00	11	0.22

Table 11. Extra performance metrics for the 18 tested Atlantic Halibut management procedures. pHealthy, pTarget and pOverfish metrics are measured in probability (proportion of simulations and time steps), and mU_Overfish is in yr^{-1}, which are defined in Table 6.

MP	Max F	Min Size Limit	pHealthy	pTarget	pOverfish	mU_Overfish
NoFish	0	81	1.00	1.00	0.00	-
conF.14_15%	0.14	81	0.00	0.00	1.00	0.20
HSfix_rampedFmsy_sl81_rel170	0.086	81	0.84	0.50	0.54	0.10
HSfix_artic1.2Fmsy_sl81_rel170	0.103	81	0.80	0.44	0.63	0.11
HSfix_rampedFmsy_sl86_rel170	0.086	86	0.81	0.44	0.66	0.10
HSfix_artic1.2Fmsy_sl86_rel170	0.103	86	0.75	0.40	0.68	0.12
HSfix_rampedFmsy_sl81_keep170	0.086	81	0.90	0.61	0.53	0.10
HSfix_artic1.2Fmsy_sl81_keep170	0.103	81	0.85	0.49	0.66	0.11
HSfix_rampedFmsy_sl86_keep170	0.086	86	0.87	0.56	0.65	0.10
HSfix_artic1.2Fmsy_sl86_keep170	0.103	86	0.81	0.45	0.71	0.12
HSrand_rampedFmsy_sl81_rel170	0.086	81	0.88	0.60	0.49	0.10
HSrand_artic1.2Fmsy_sl81_rel170	0.103	81	0.88	0.50	0.63	0.11
HSrand_rampedFmsy_sl86_rel170	0.086	86	0.86	0.56	0.65	0.10
HSrand_artic1.2Fmsy_sl86_rel170	0.103	86	0.84	0.45	0.68	0.11
HSrand_rampedFmsy_sl81_keep170	0.086	81	0.93	0.68	0.49	0.10
HSrand_artic1.2Fmsy_sl81_keep170	0.103	81	0.90	0.55	0.66	0.11
HSrand_rampedFmsy_sl86_keep170	0.086	86	0.90	0.64	0.64	0.10
HSrand_artic1.2Fmsy_sl86_keep170	0.103	86	0.87	0.49	0.72	0.11

FIGURES

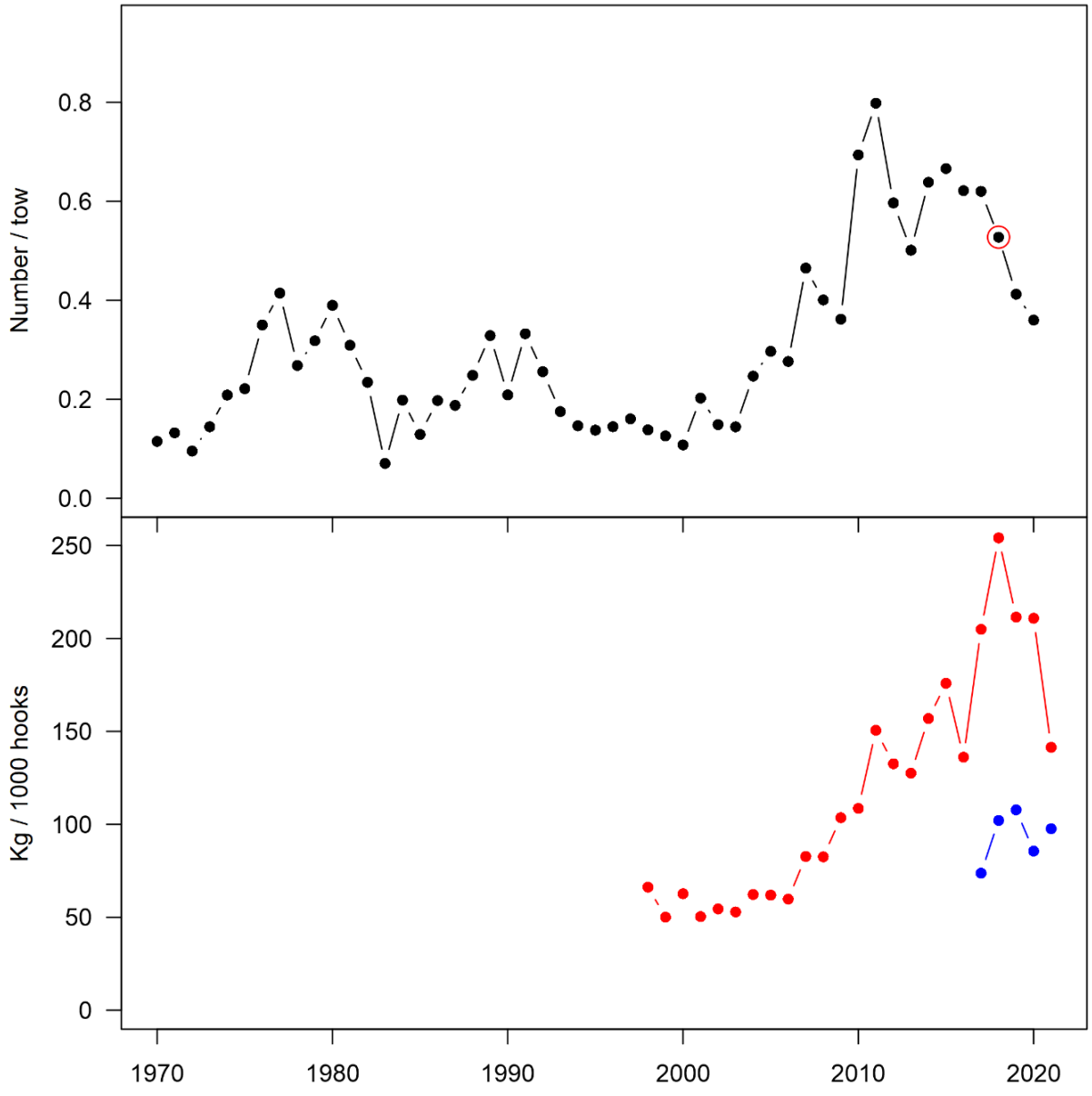

Figure 1. Indices of abundance used to fit the SISCAL model. Top is number per tow from Maritimes Summer Ecosystem Research Vessel Survey, red circles indicates 2018 where the survey only covered 4X. Bottom are the biomass indices in Kg / 1000 hooks from the fixed station (red) and stratified random (blue) longline Halibut surveys.

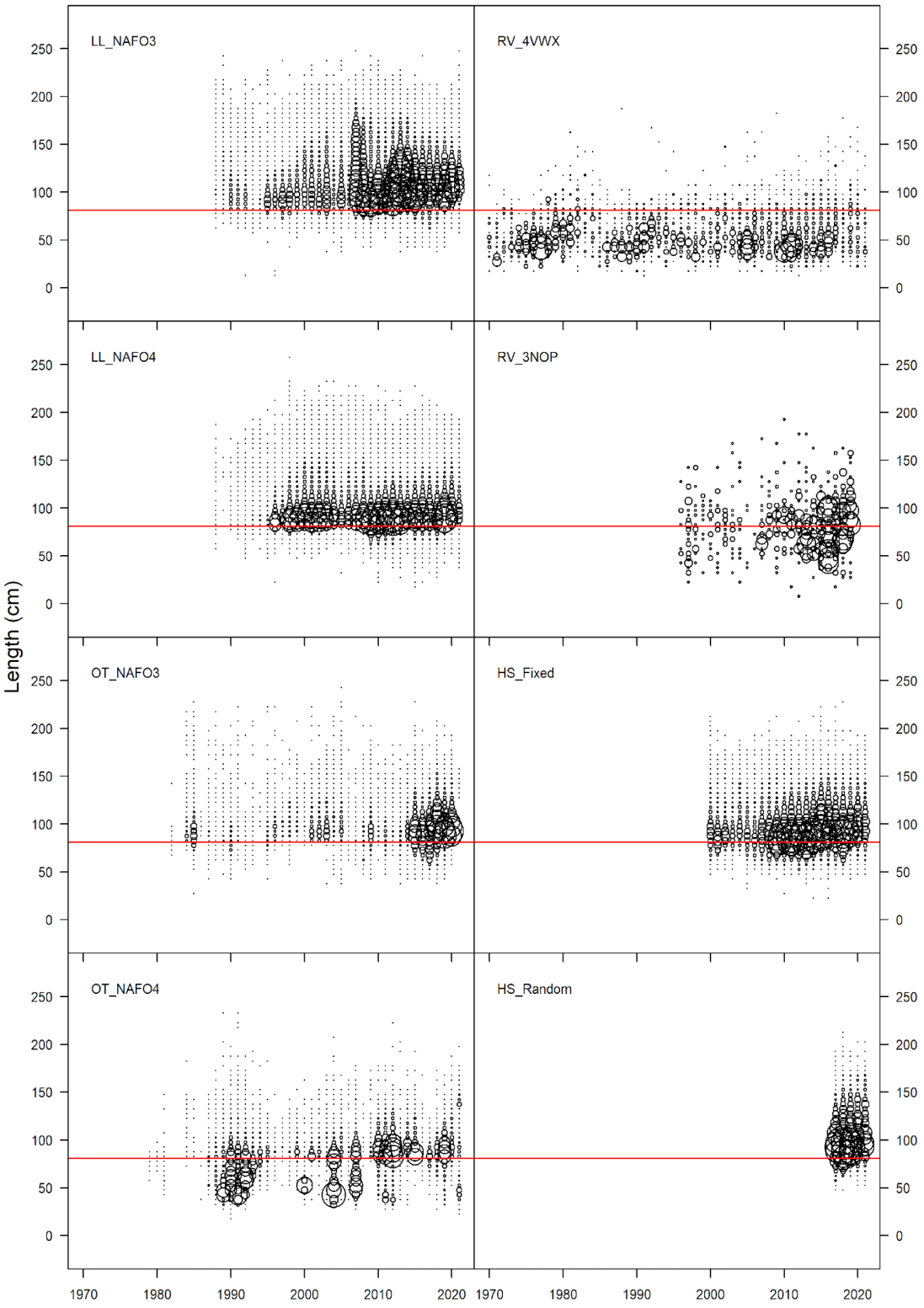

Figure 2. Length Composition data from the 4 fleets (left column) and 3 indices of abundance (right column). Red line indicates min legal size (81 cm).

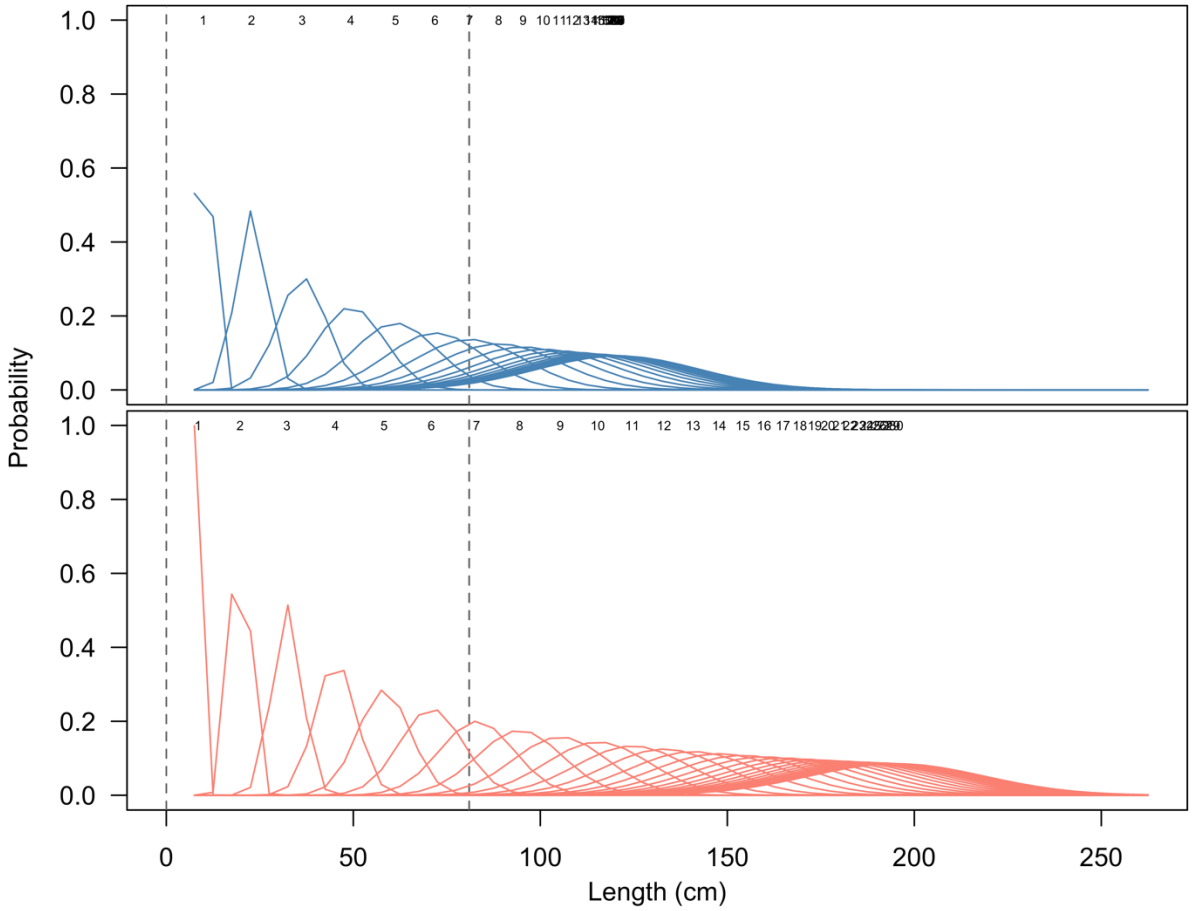

Figure 3. Length-at-age distributions derived from growth parameters for males (top) and females (bottom).

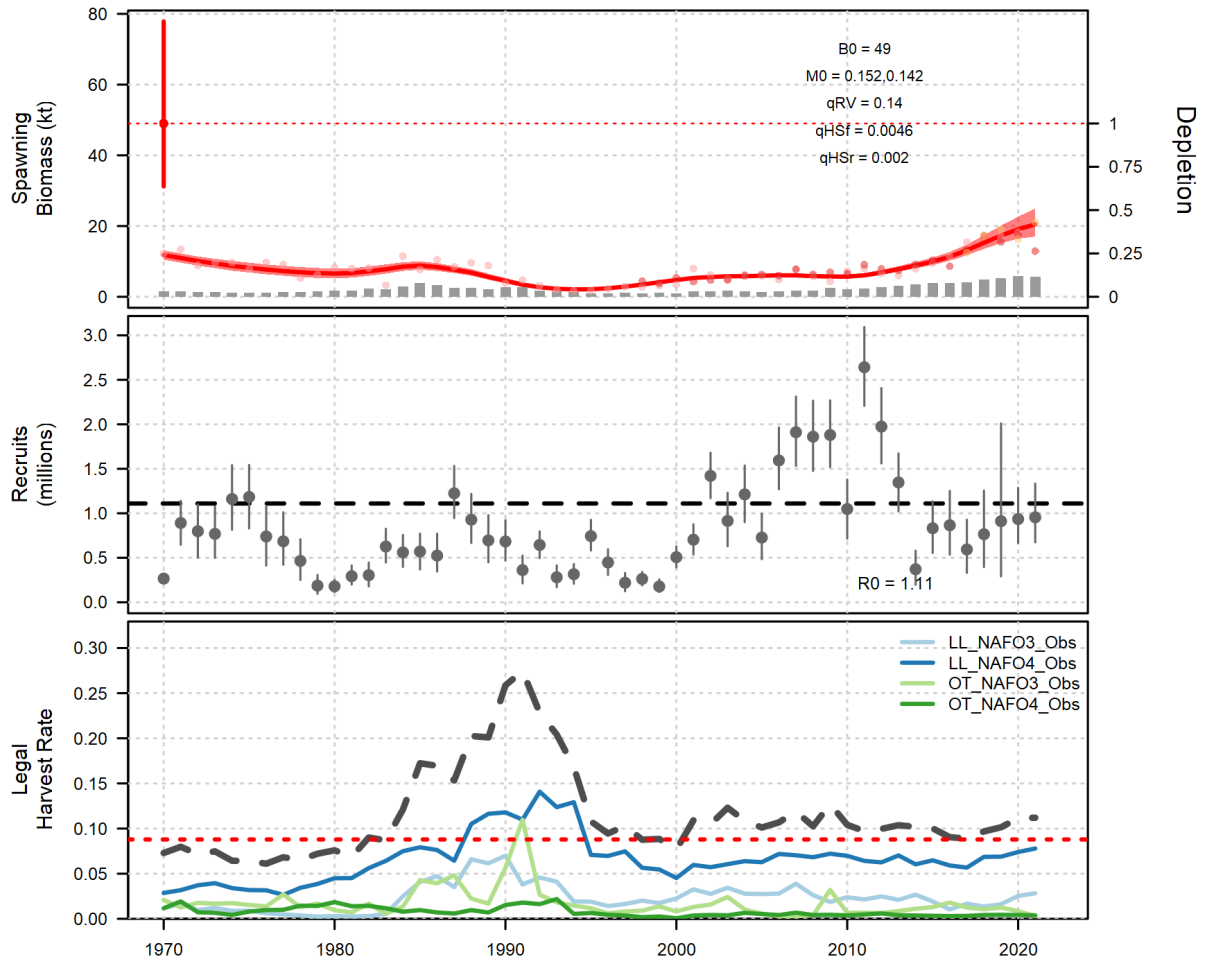

Figure 4. Time series of spawning biomass with scaled spawn indices (top), recruitments (second row), and harvest rates (bottom row) for areas of Atlantic halibut. Catch bars in the top panel show landings only (not releases). The vertical line segment in the top panel shows the posterior 95% credibility interval for unfished biomass.

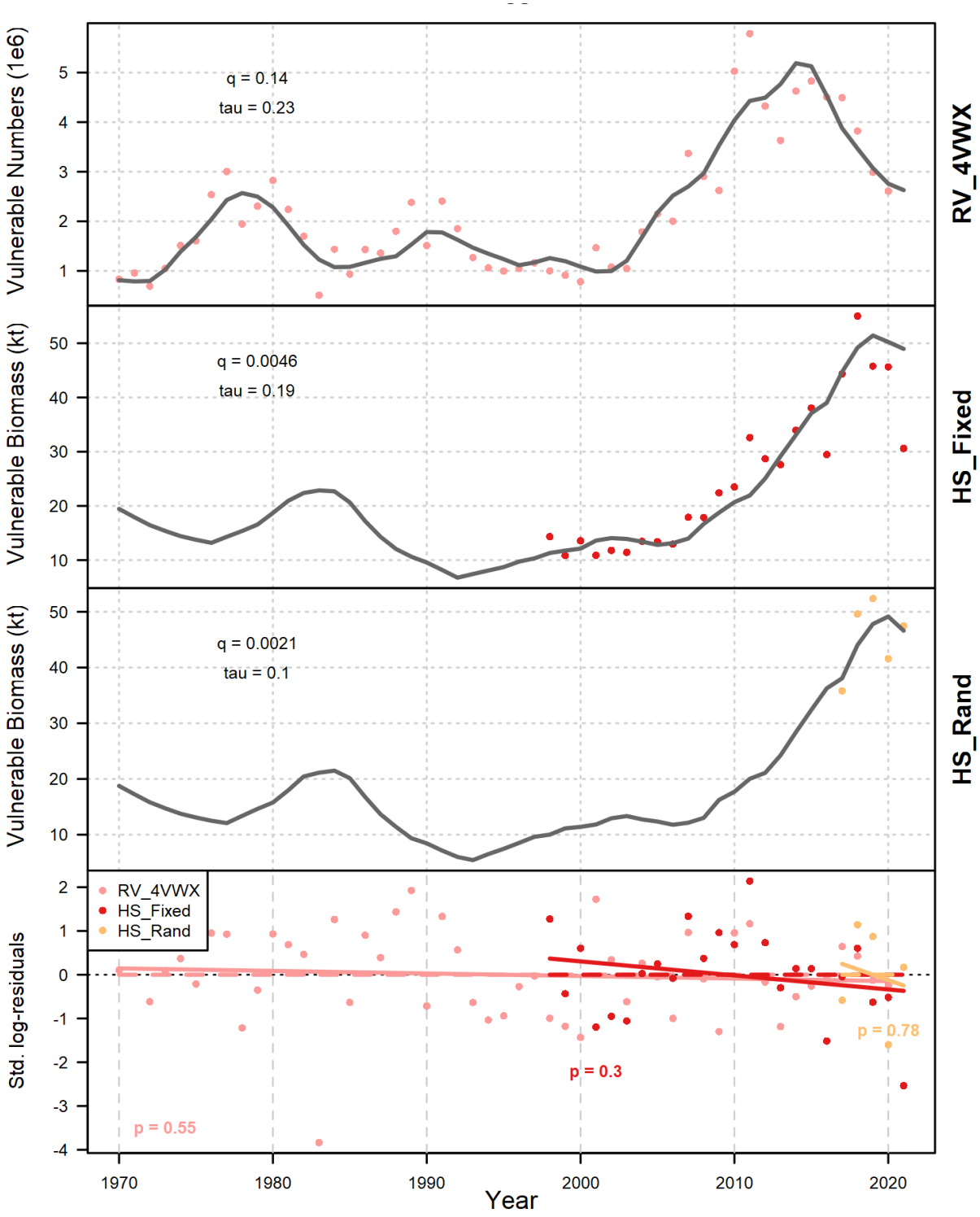

Figure 5. Model fits to abundance and biomass indices Maritimes Summer Ecosystem Research Vessel Survey (top), fixed station portion of the Industry-DFO Halibut Longline Survey (second), stratified random portion of the Industry-DFO Halibut Longline Survey (third) and the standardised log residuals where the significance of the linear fit to the residuals (p-value) is reported for each of the three surveys(bottom panel).

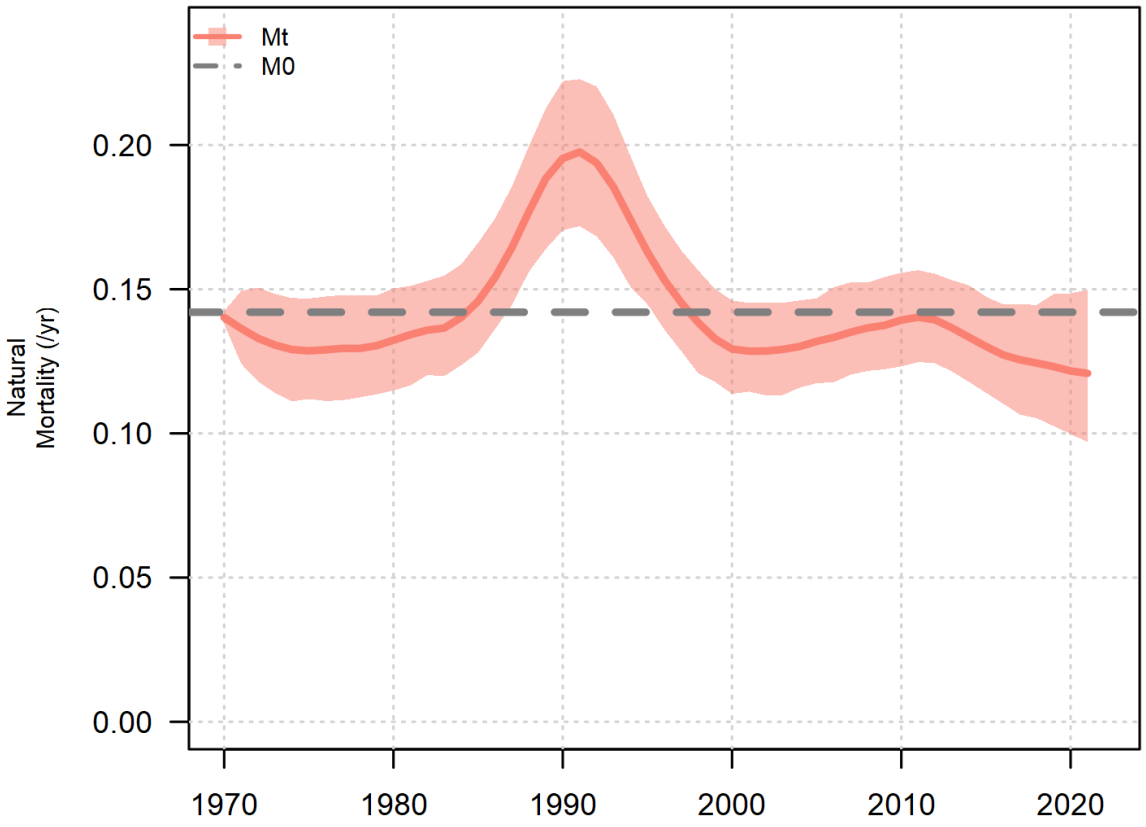

Figure 6. Posterior mean and 95% credibility intervals for estimates of time-varying natural mortality (Mt) compared to the initial prior (M0).

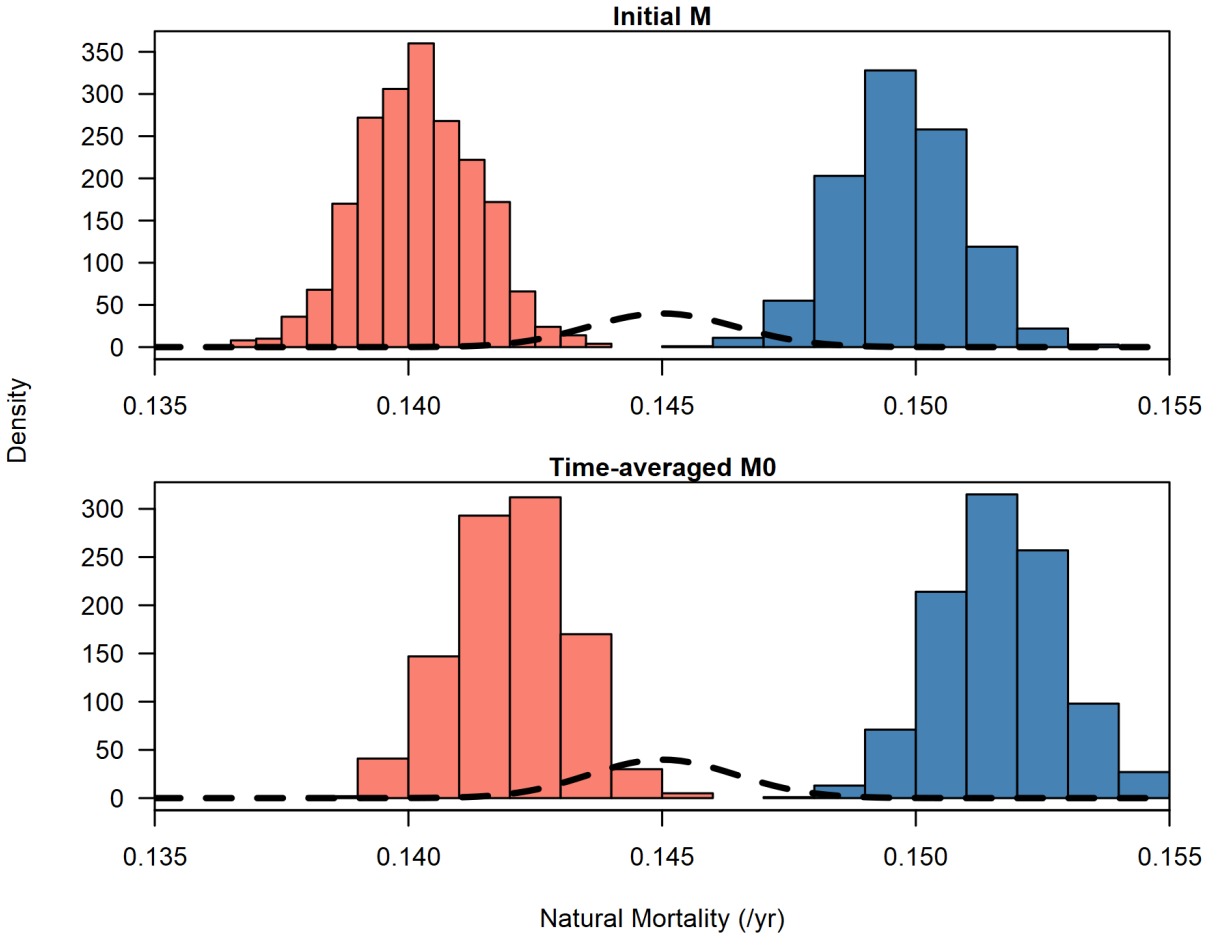

Figure 7. Prior (line) and posterior (bars) density of initial M (top) and time-averaged M (bottom) for males (blue) and females (red).

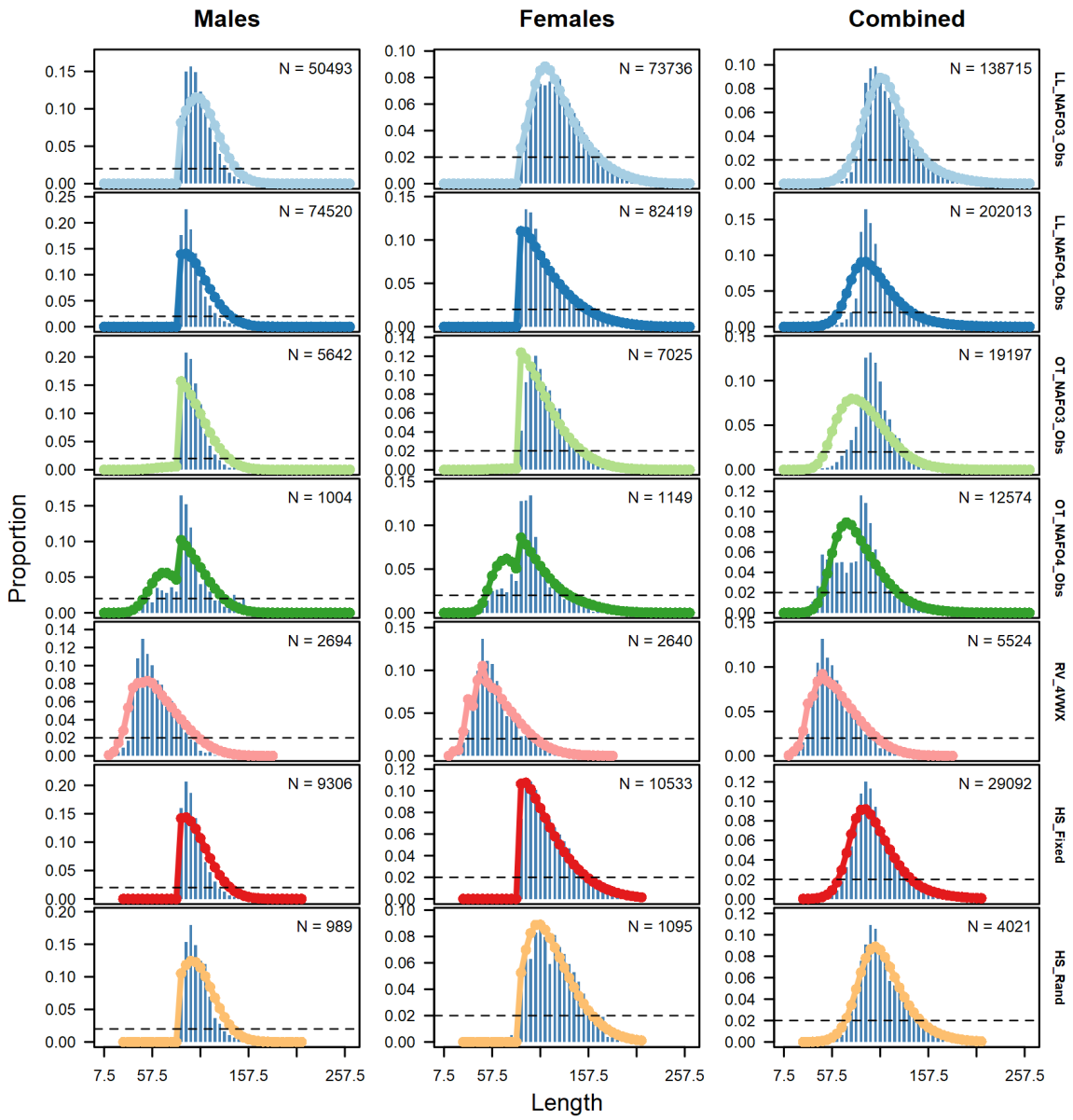

Figure 8. Time-averaged model fits to length composition data. Sexes/stocks are left to right, and gears are top to bottom.

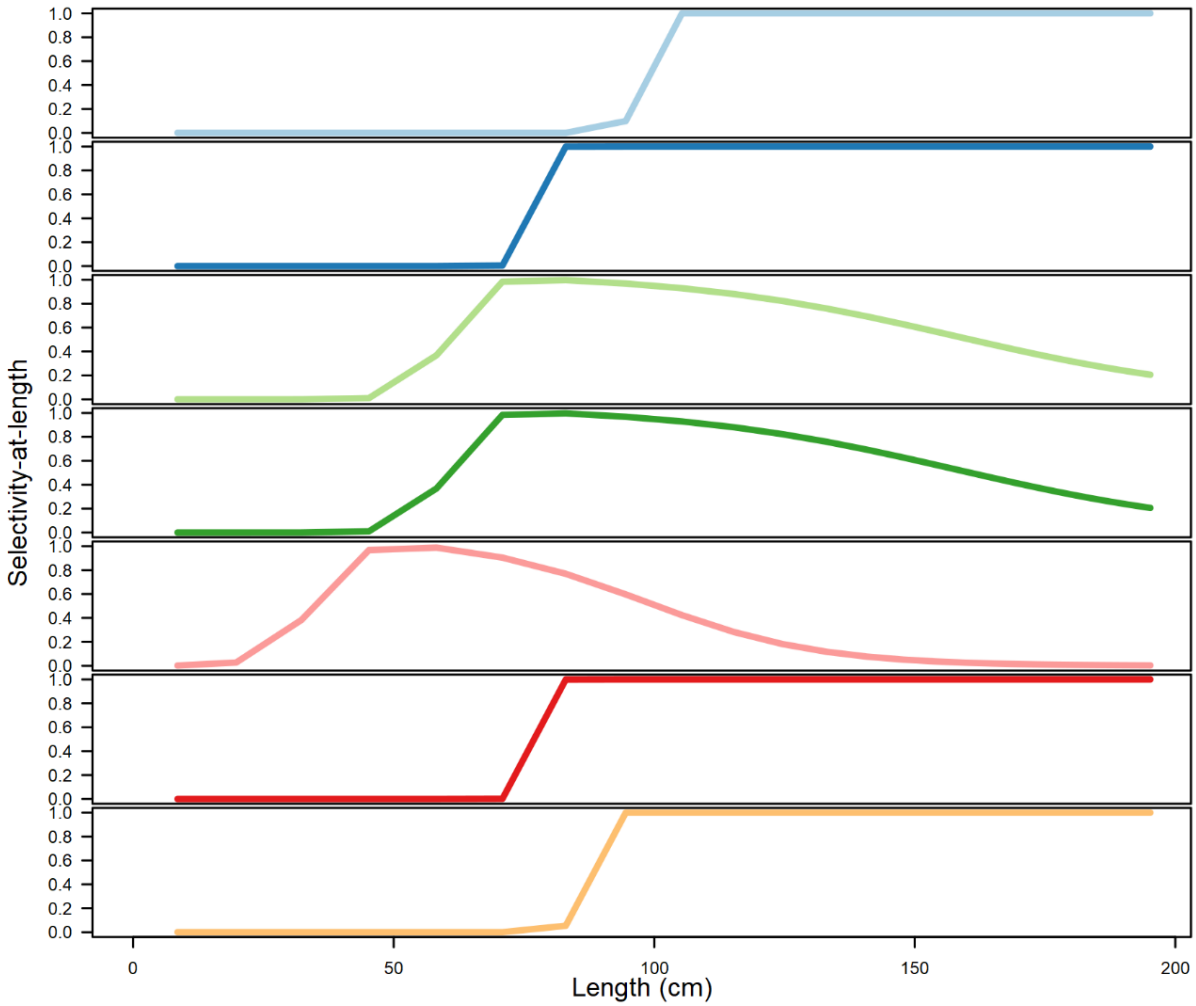

Figure 9. Selectivity-at-length for each fleet (top to bottom: Longline 3NOP, Longline 4VWX5Zc, Otter trawl 3NOP, Otter trawl 4VWX5Zc, RV survey 4VWX, fixed station portion and the random stratified portion of the Industry-DFO Halibut Longline Survey).

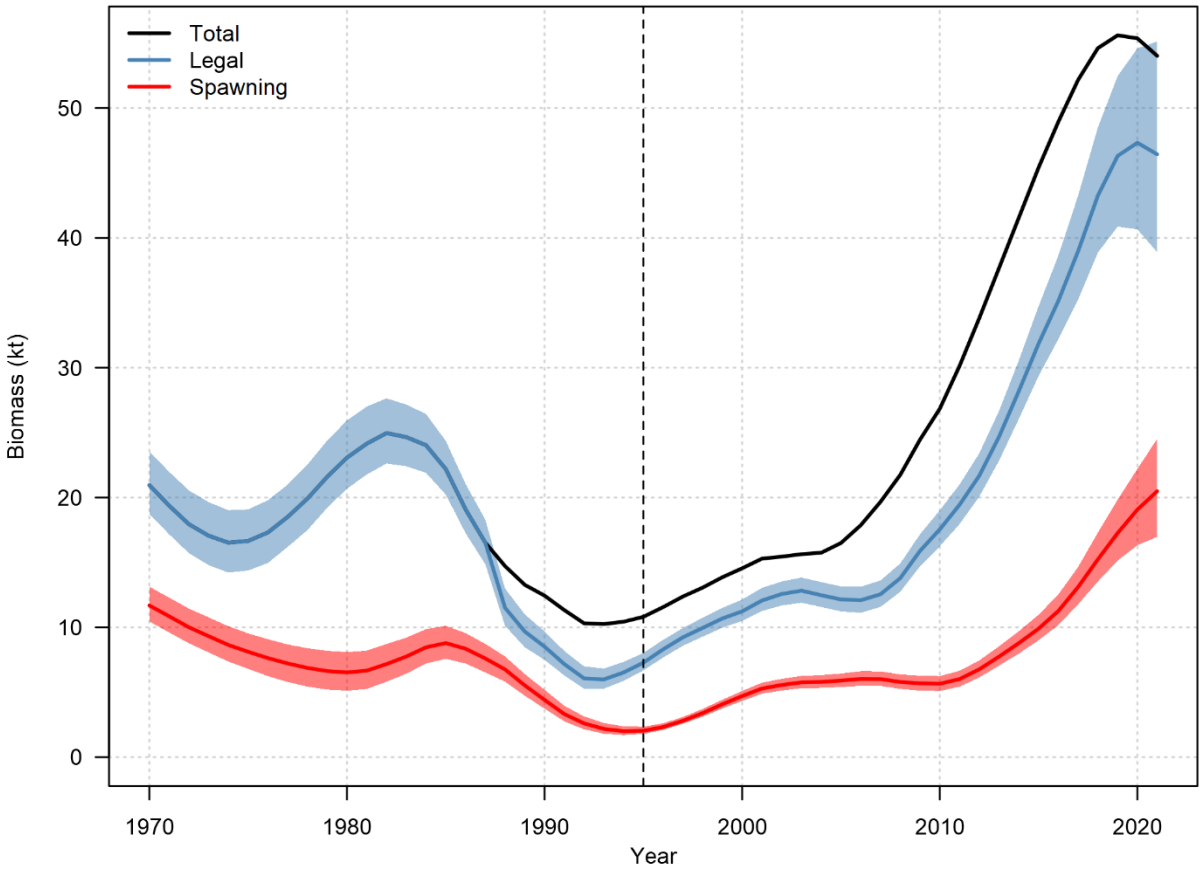

Figure 10. Posterior mean and 95% credibility intervals of legal (<81cm) and spawning biomass, and posterior mean total Atlantic Halibut biomass. The vertical dashed line shows 1995, the year where the minimum size limit was fully established in all fleets.

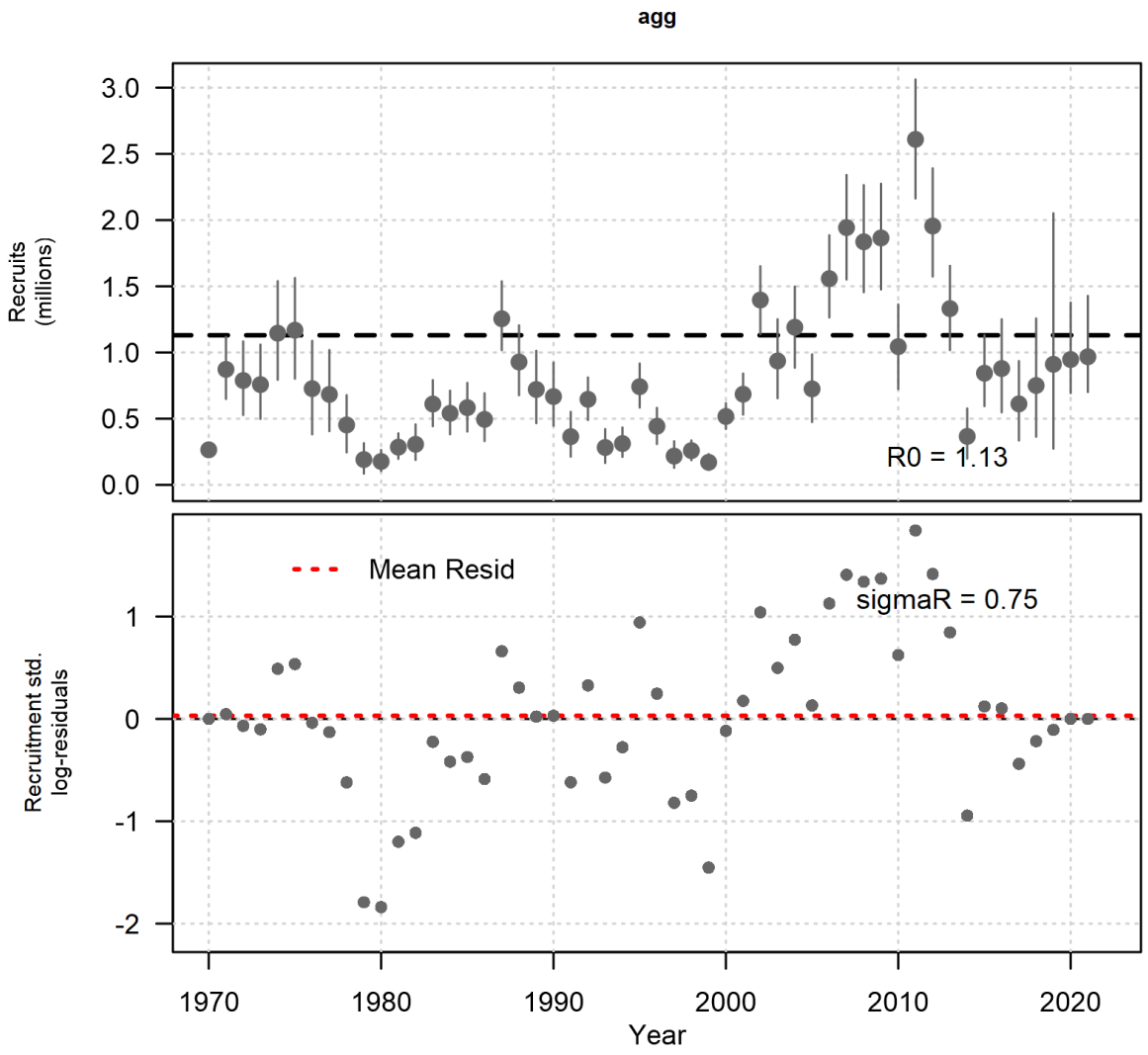

Figure 11. Age-1 recruitments for all stocks. Equilibrium unfished recruitment R_0 is indicated by the horizontal dashed line. Second row shows recruitment residuals on the log scale, with the average of estimated residuals shown by the horizontal red dashed line.

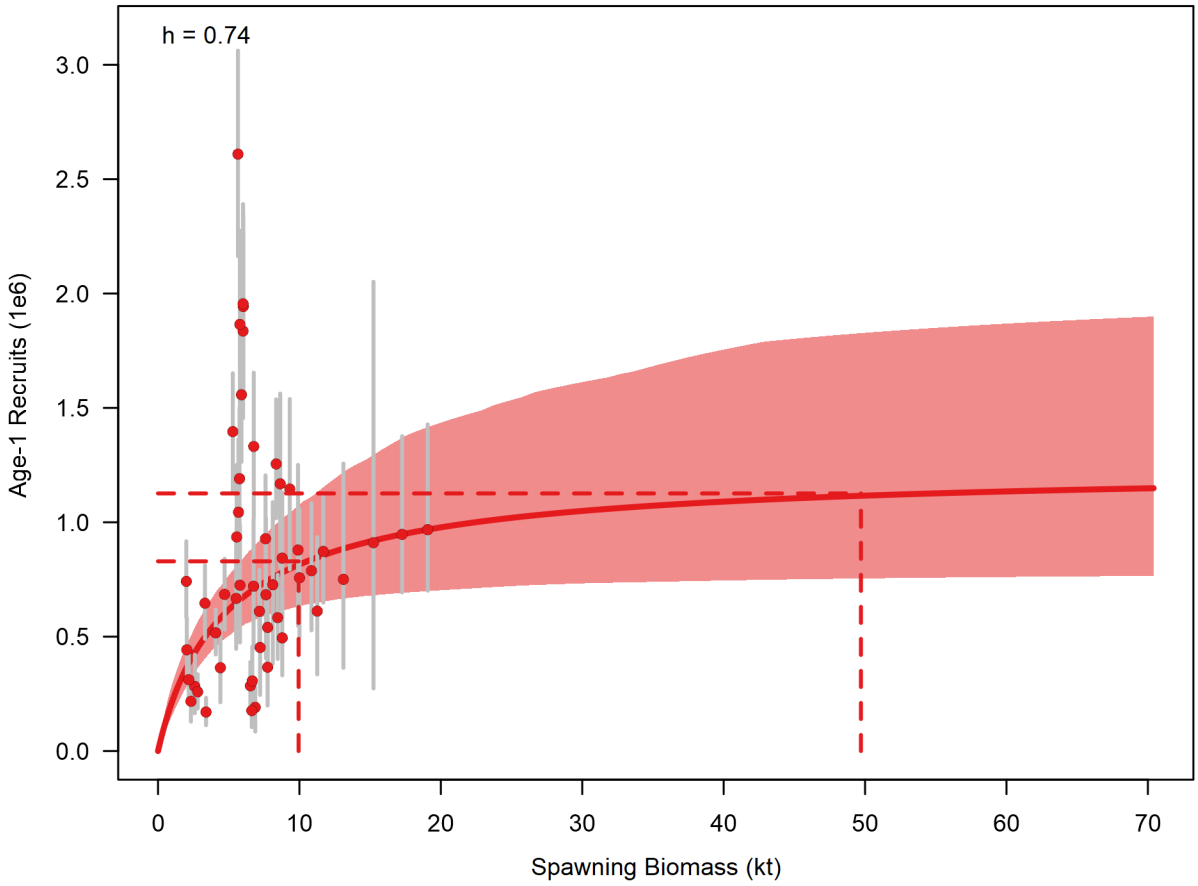

Figure 12. Stock-recruit curve (solid line and red envelope) and modeled recruitments (red points with grey credibility intervals).

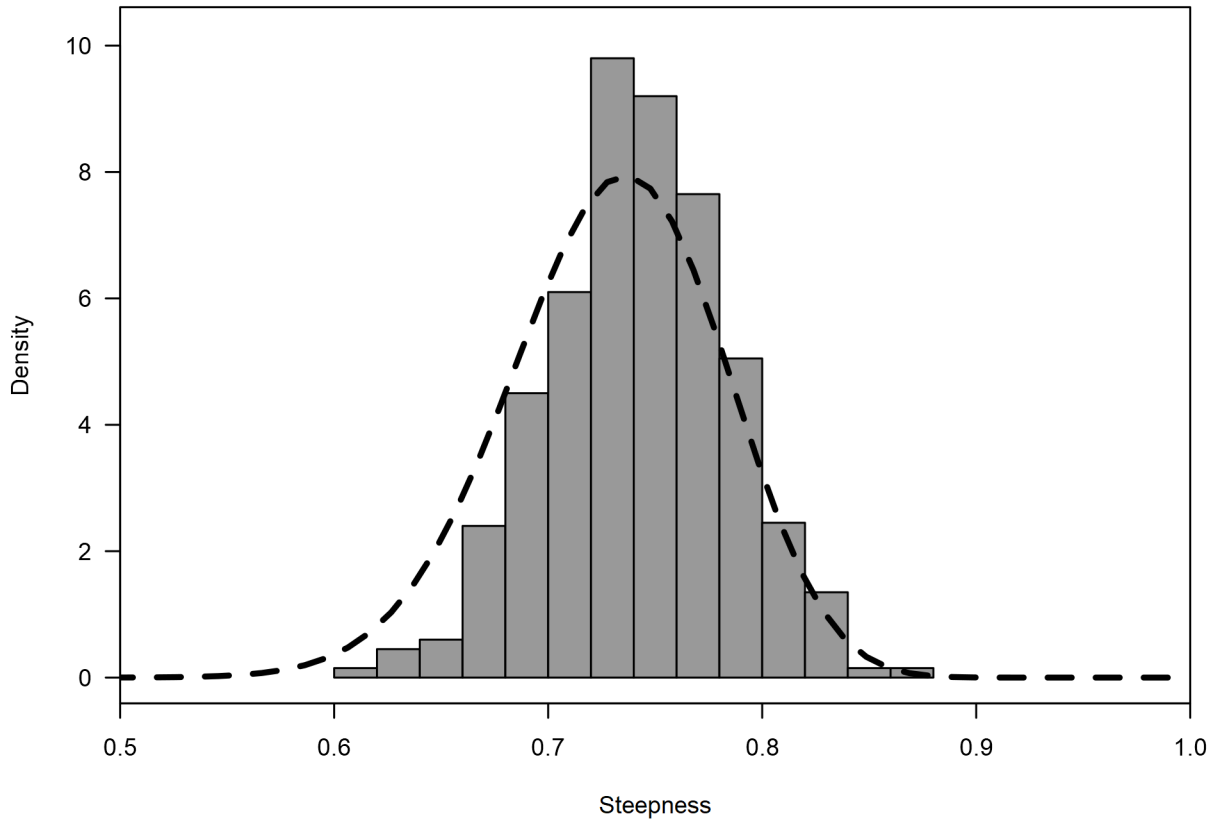

Figure 13. Prior (line) and posterior (bars) density of stock-recruit steepness.

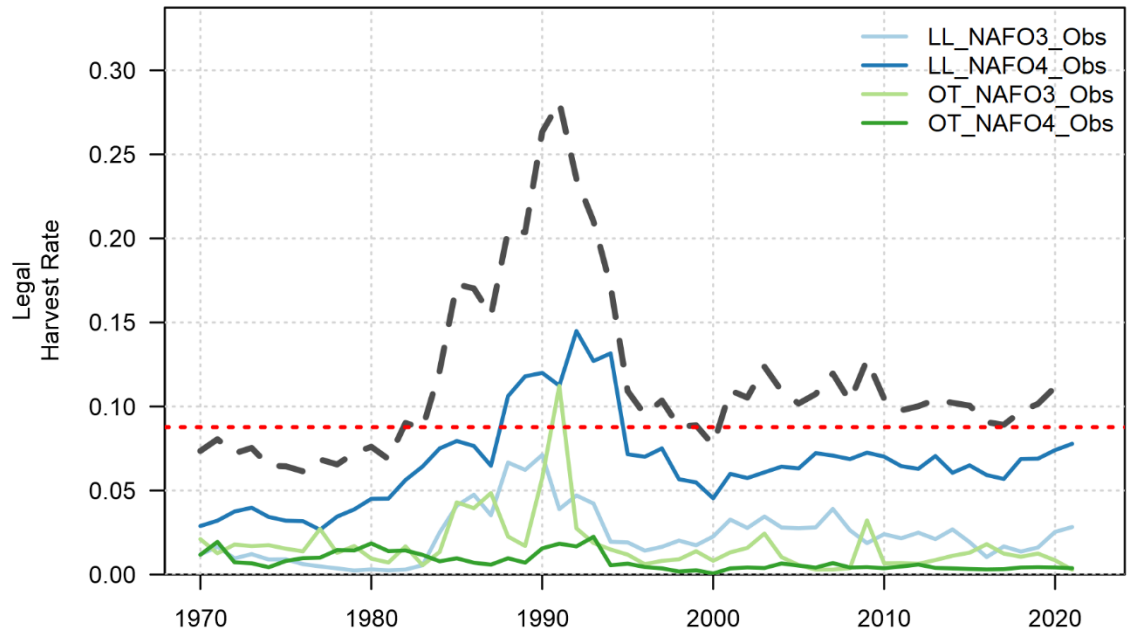

Figure 14. Time series of harvest rate for each fleet. Dashed black line is overall harvest rate and the dotted red line is U_{MSY}.

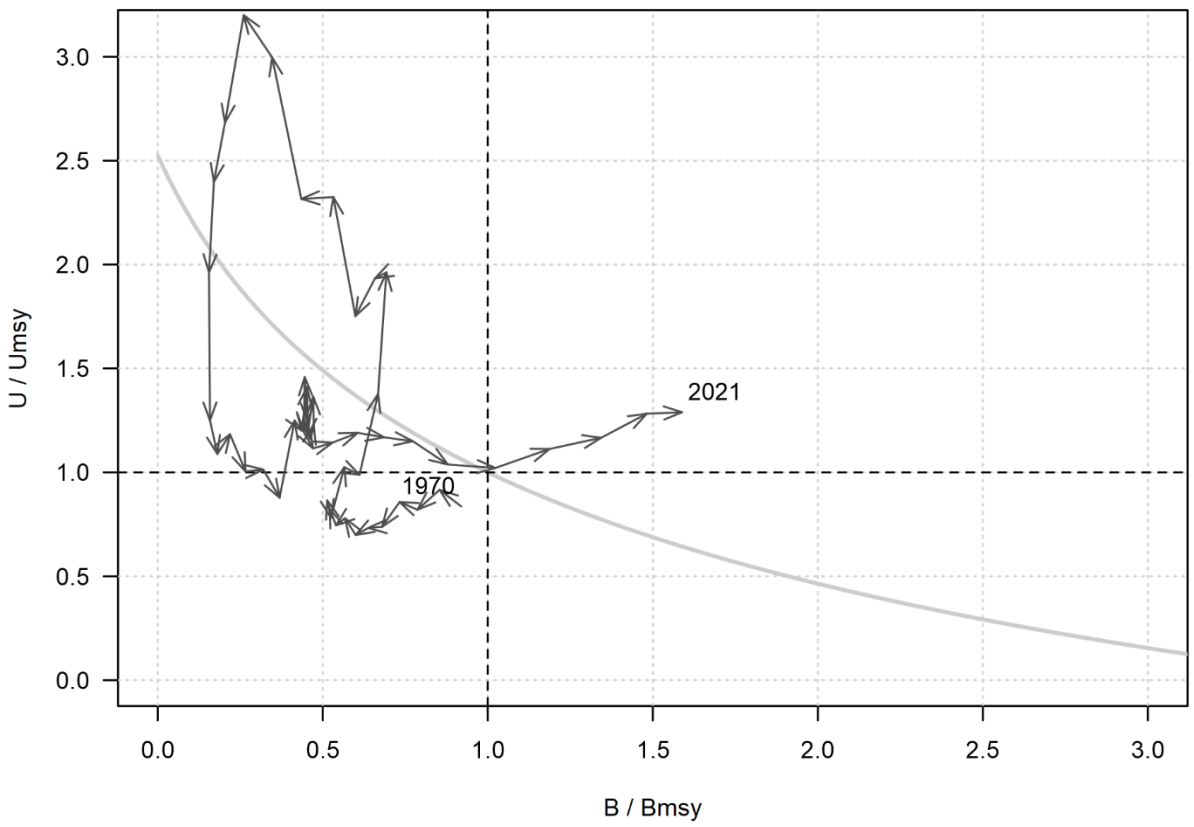

Figure 15: Phase plot showing spawning biomass (vertical axis) and total legal harvest rate (horizontal axis) relative to U_{MSY} reference points. Arrows show the direction of time, beginning in 1970 and ending in 2020. Equilibrium spawning biomass is shown as a faint grey curve in the background of the plot.

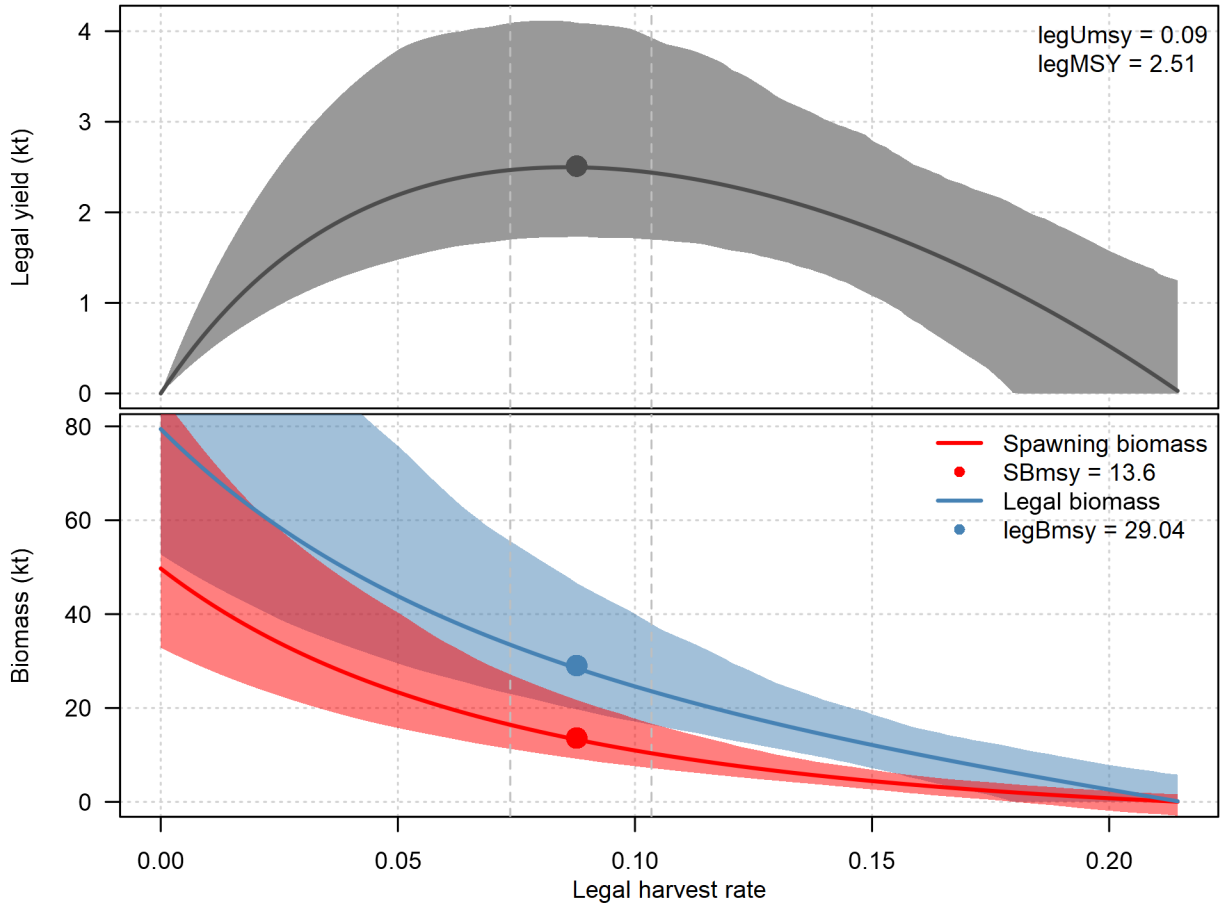

Figure 16. Equilibrium yield (top) and biomass (bottom) curves as a function of total legal harvest rates. U_{MSY} reference points are shown as closed circles on each line. Posterior 95% credibility intervals in yield and biomass are shown as envelopes, while the 95% credibility interval for legal U_{MSY} is shown by the vertical dashed lines.

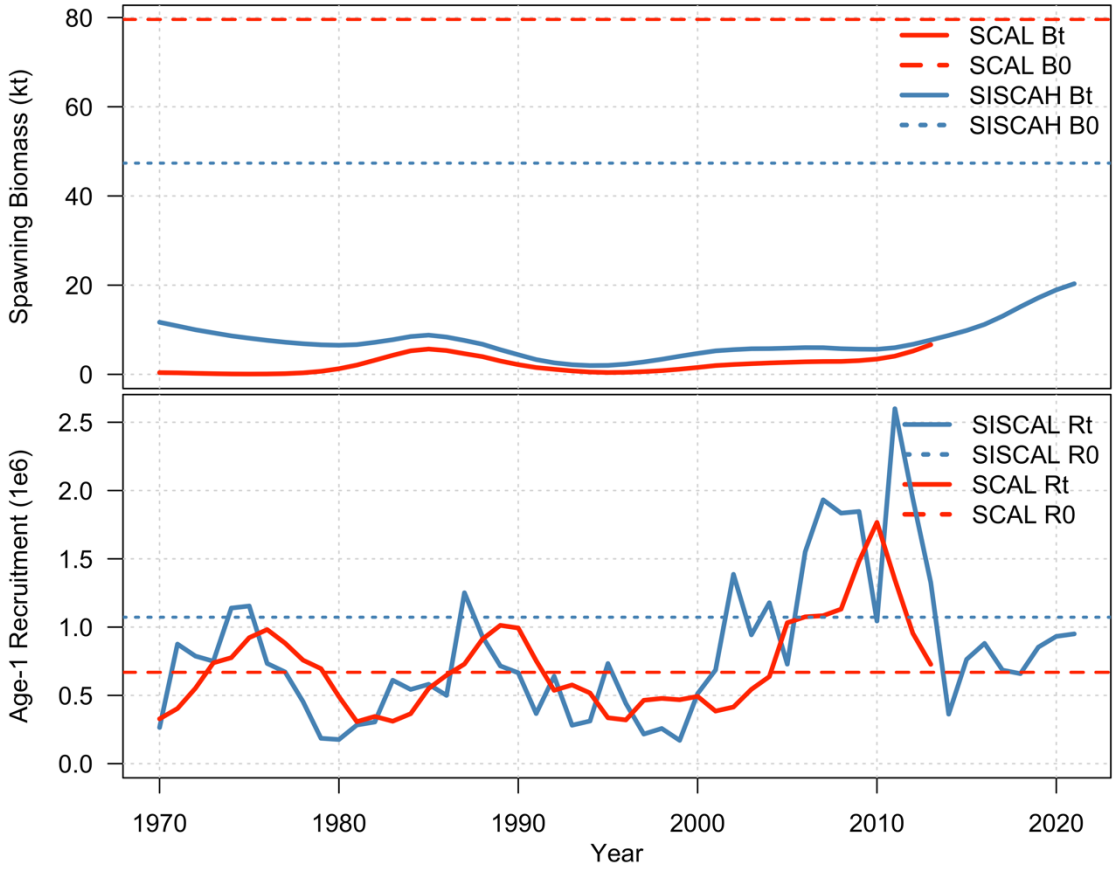

Figure 17. Comparison of spawning stock biomass and age-1 recruitment at the major stock level between SCAL and SISCAL.

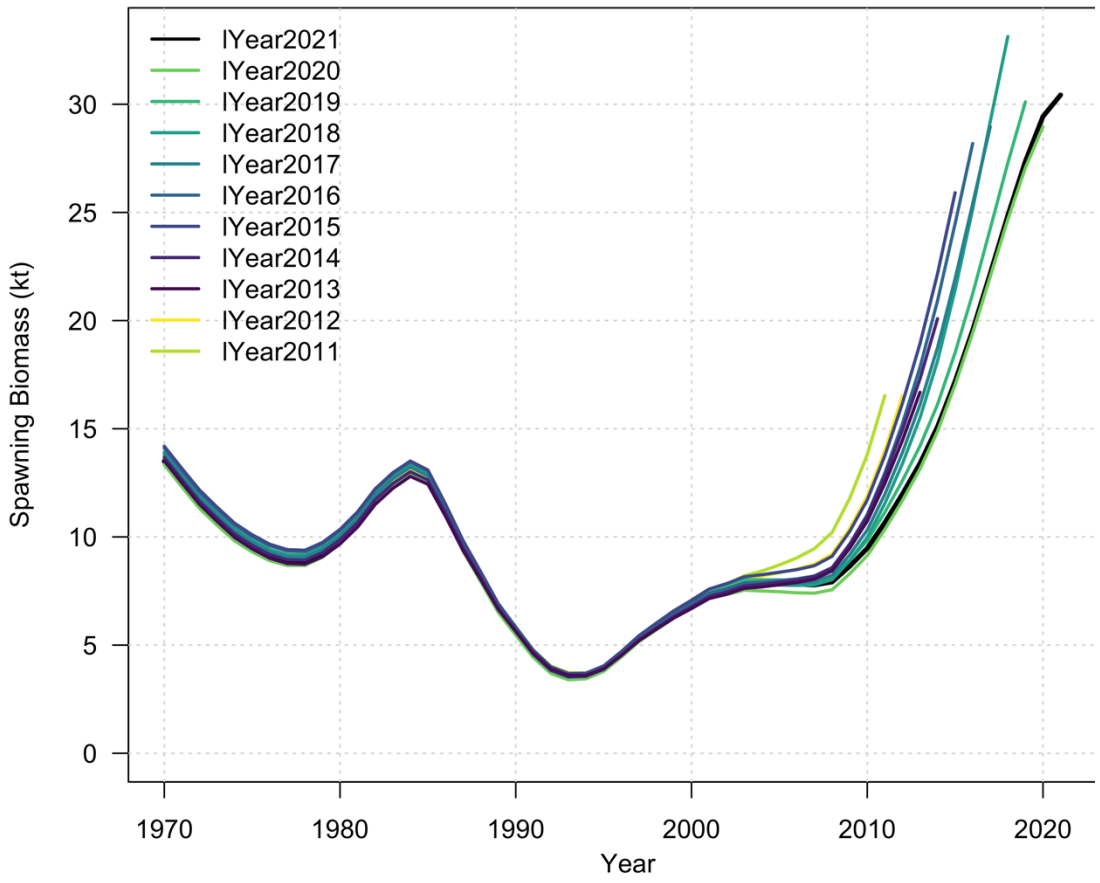

Figure 18. A retrospective analysis that shows spawning biomass when the model is fit with 2011 through 2021 as the final year.

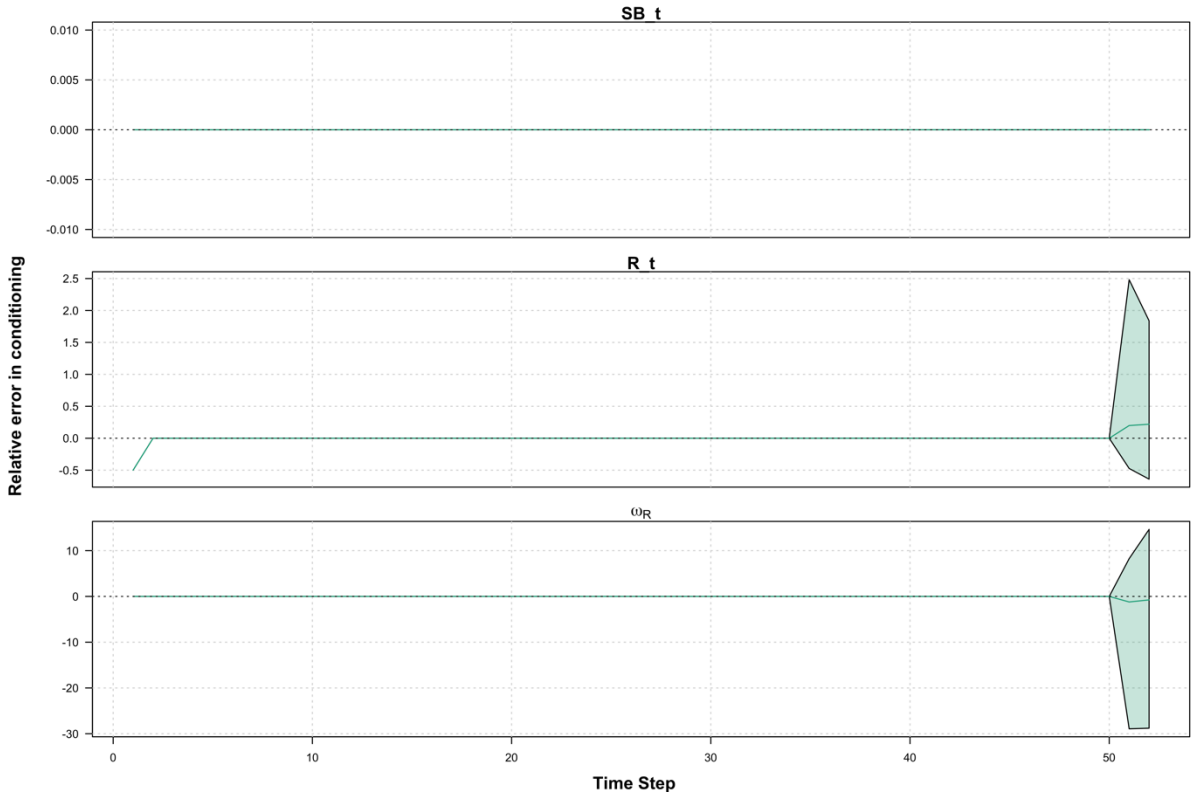

Figure 19. Relative error between ms3-HAL and SISCAL-AH time series of spawning biomass (SB_t), recruitment (R_t), and recruitment process error deviations (ω_R). Each plot shows a polygon representing the central 95% of relative errors across 100 random posterior draws, with a solid green line showing the median error. High relative errors in recruitments and process errors indicate where SISCAL-AH was unable to estimate recruitments during optimisation.

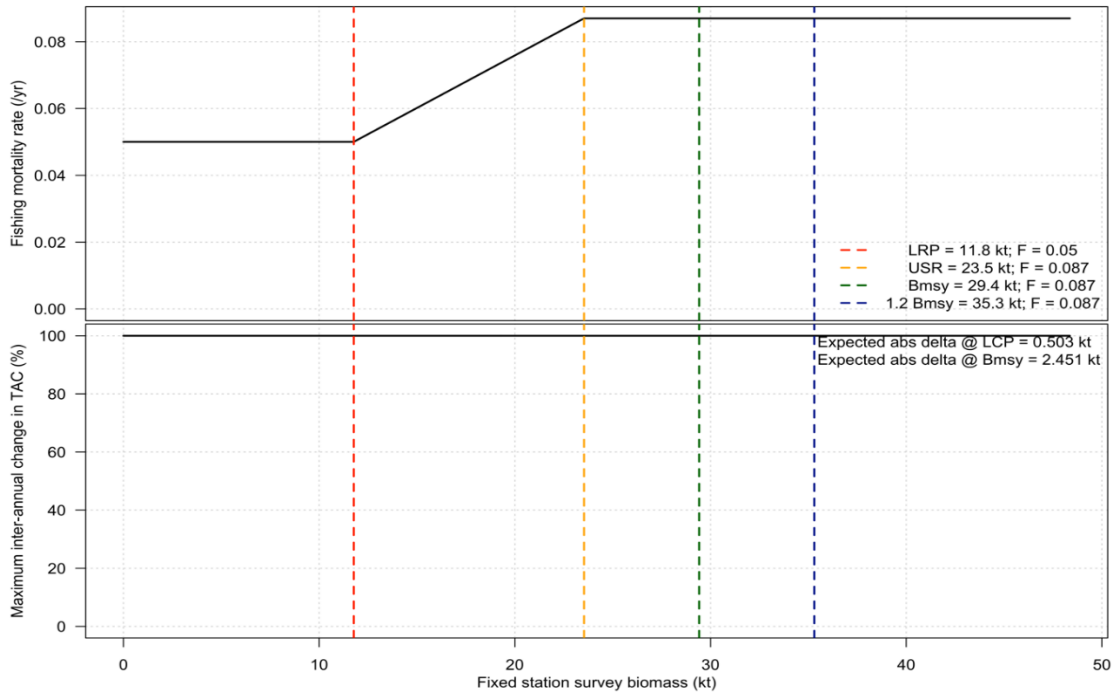

Figure 20. The rampedFmsy harvest control rule used for determining target harvest rates for Atlantic Halibut based on estimates of survey biomass. This example is for management procedures using fixed station portion of the Industry-DFO Halibut Longline Survey biomass for estimating stock status.

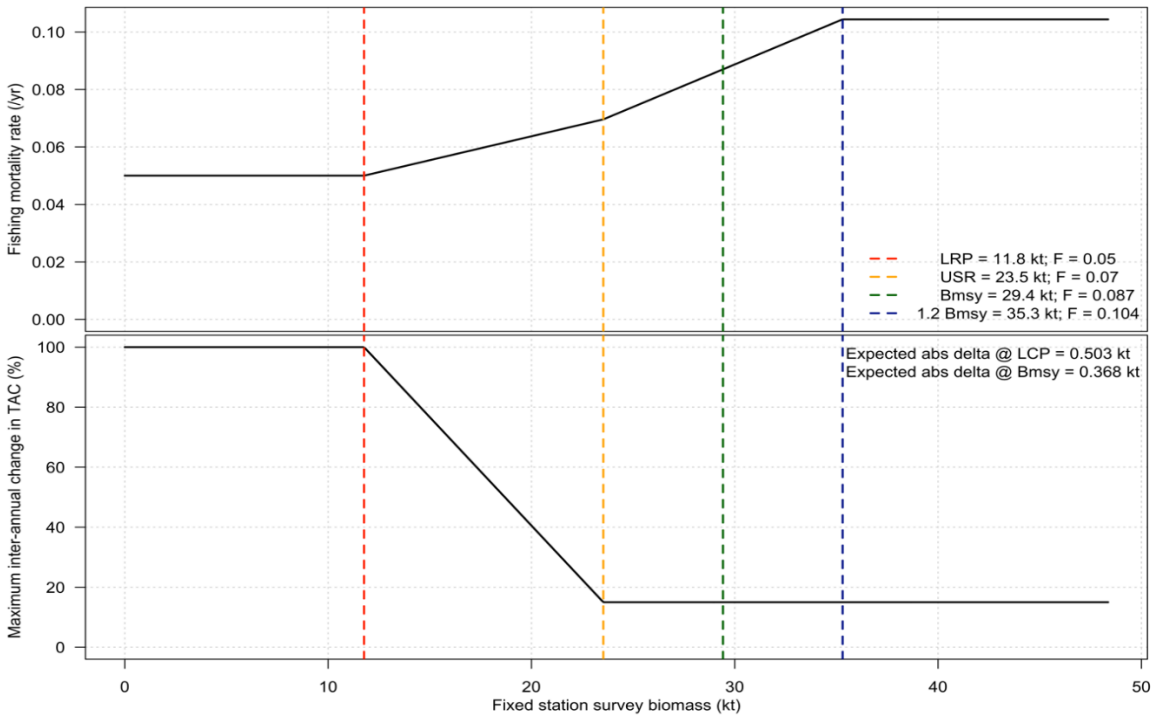

Figure 21. The artic1.2Fmsy harvest control rule used for determining target harvest rates for Atlantic Halibut based on estimates of survey biomass. This example is for management procedures using fixed station portion of the Industry-DFO Halibut Longline Survey survey biomass for estimating stock status.

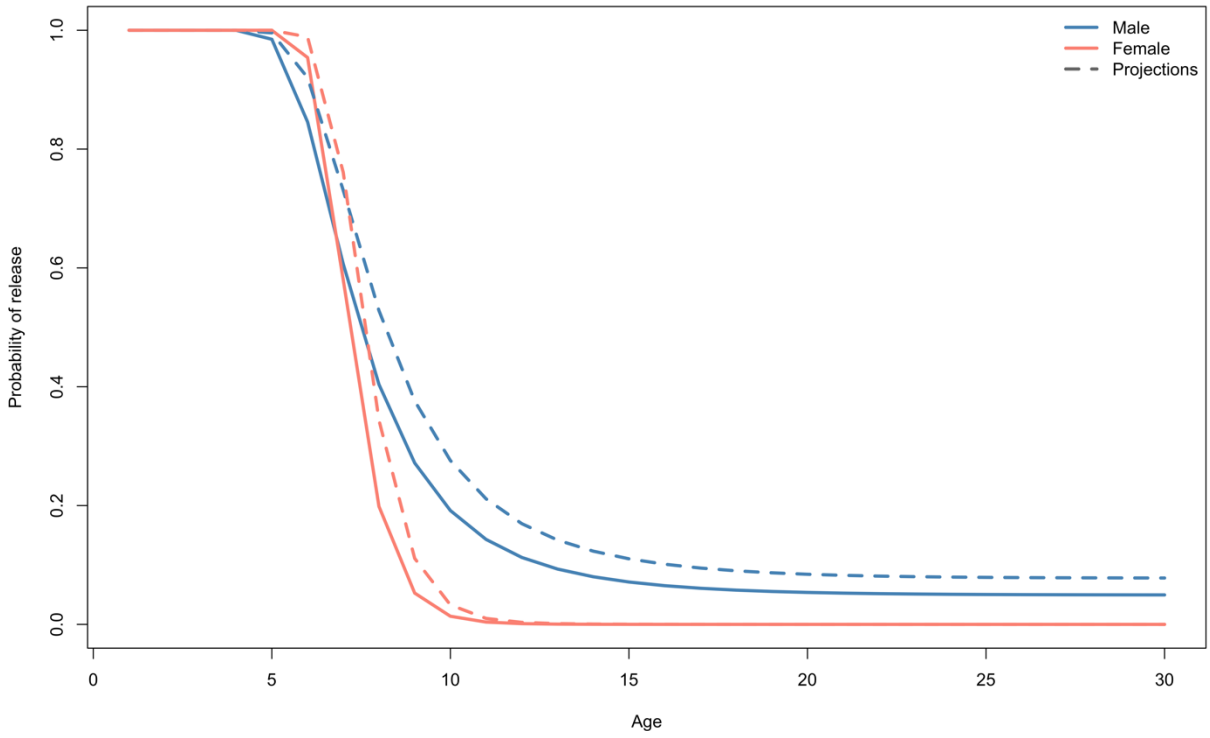

Figure 22. Probability of release at each age under an 81 cm legal minimum size limit (solid lines) and an 86 cm size limit (dashed lines).

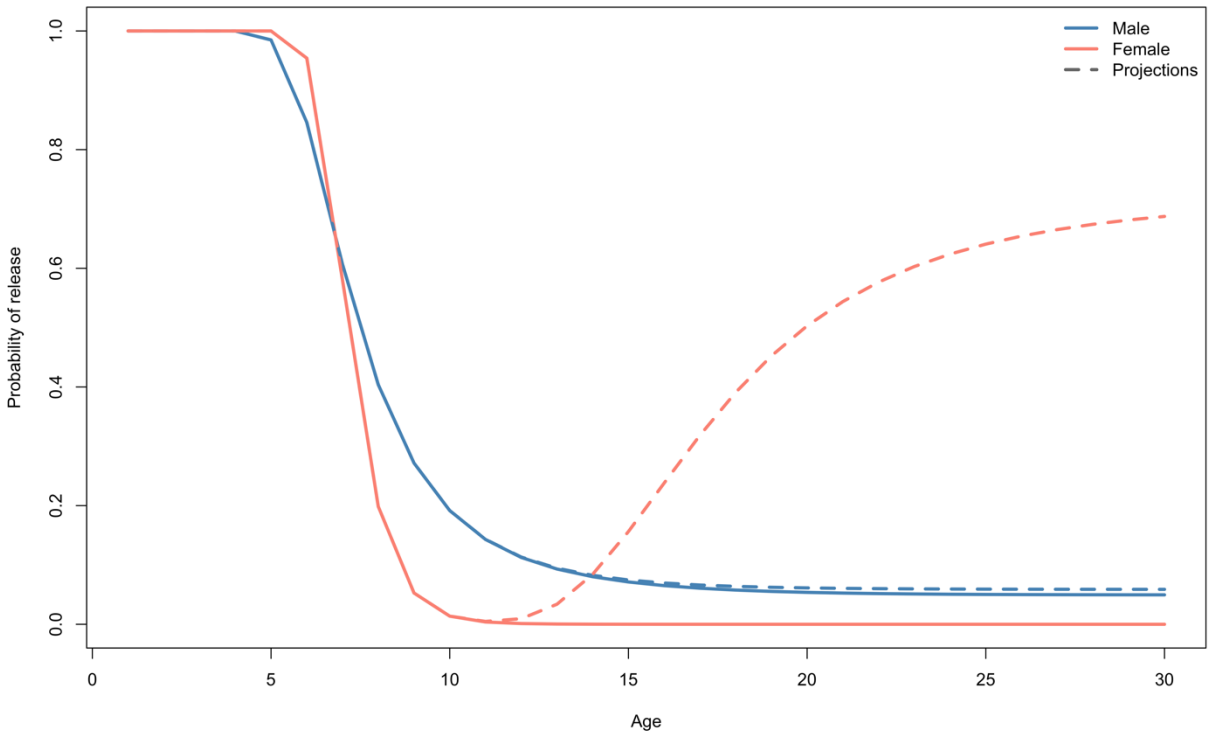

Figure 23. Probability of release at each age under an 81 cm legal minimum size limit (solid lines) and an additional 80% release rate for fish greater than 170 cm in length (dashed lines).

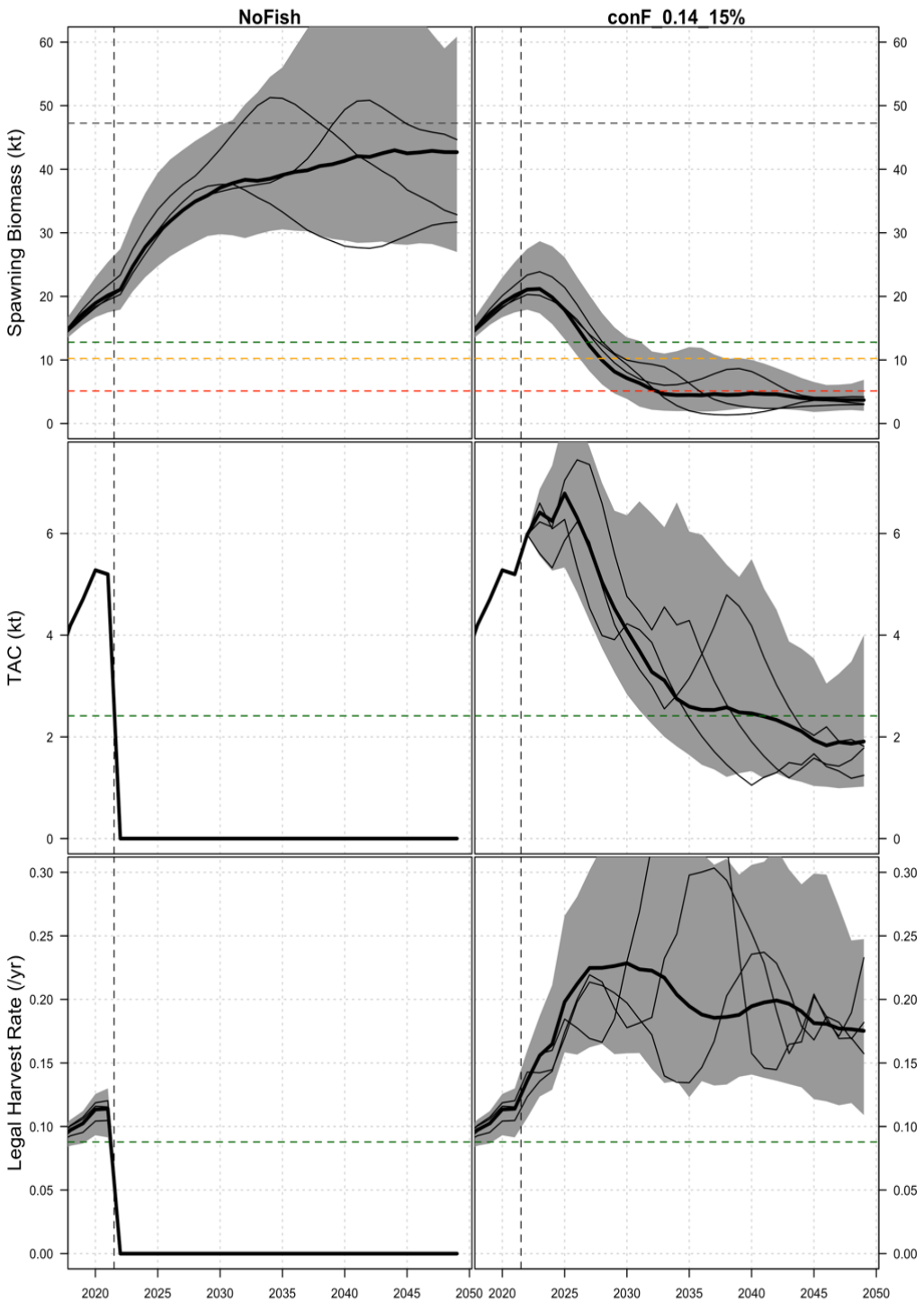

Figure 24. Simulation envelopes for spawning biomass (top row), total allowable catch (TAC, middle row), and realised fishing mortality rate (bottom row) for 2022 – 2050 for the No Fishing procedure (left) and the current conF_0.14_15% procedure (right). Envelopes represent the central 95% (grey) of outcomes, median (50% above/below; thick black line), and spaghetti traces (thin lines) showing 3 randomly chosen example outcomes. Horizontal dashed reference lines show B_{MSY} (top, green), 0.8 B_{MSY} (top, yellow), and the limit reference point of 0.4 B_{MSY} (top, red), MSY (middle, green), and legal U_{MSY} (bottom).

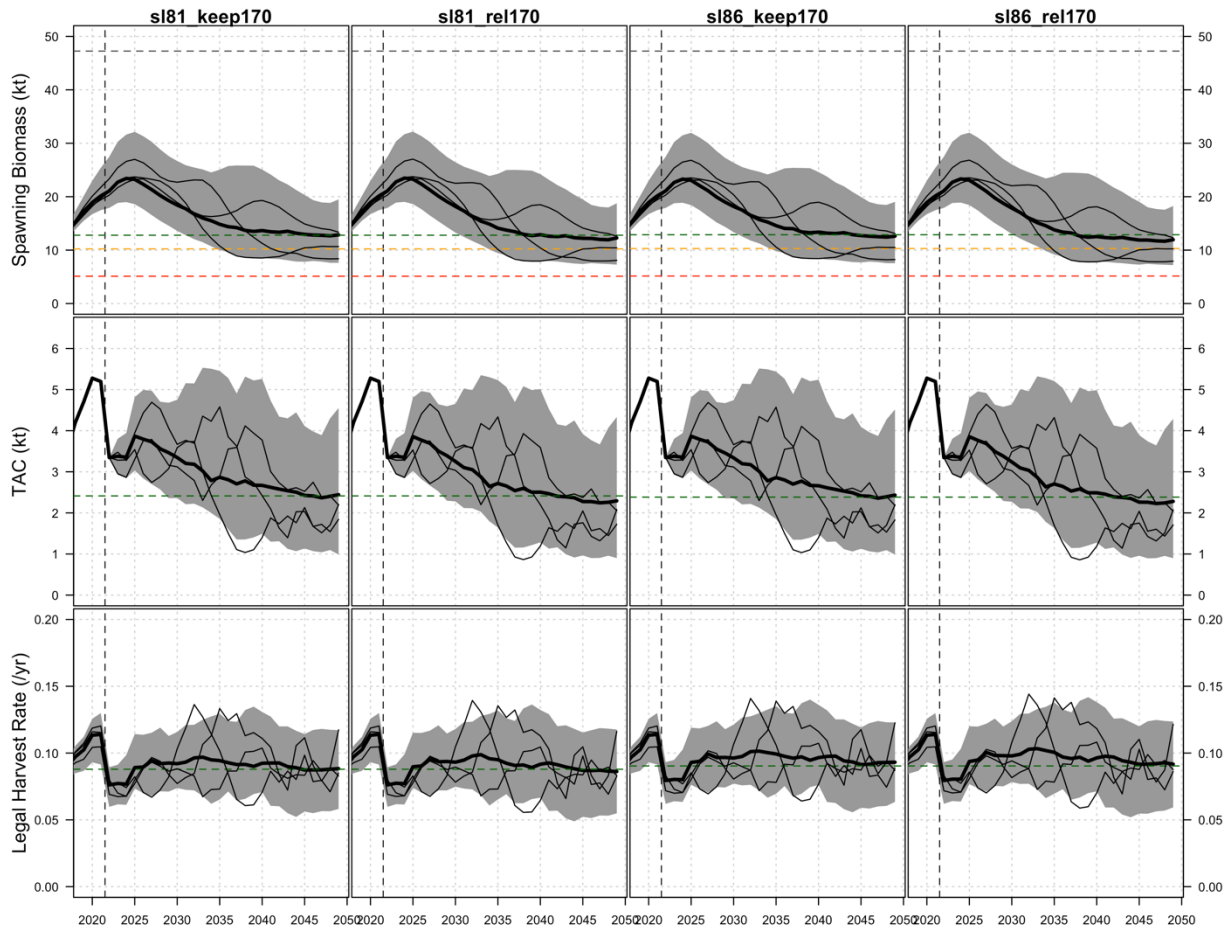

Figure 25. Simulation envelopes for spawning biomass (top row), total allowable catch (TAC, middle row), and realised fishing mortality rate (bottom row) for 2022 – 2050 under fixed station survey with the rampedFmsy harvest control rule. Envelopes represent the central 95% (grey) of outcomes, median (50% above/below; thick black line), and spaghetti traces (thin lines) showing 3 randomly chosen example outcomes. Horizontal dashed reference lines show B_{MSY} (top, green), 0.8 B_{MSY} (top, yellow), and the limit reference point of 0.4 B_{MSY} (top, red), MSY (middle, green), and legal U_{MSY} (bottom).

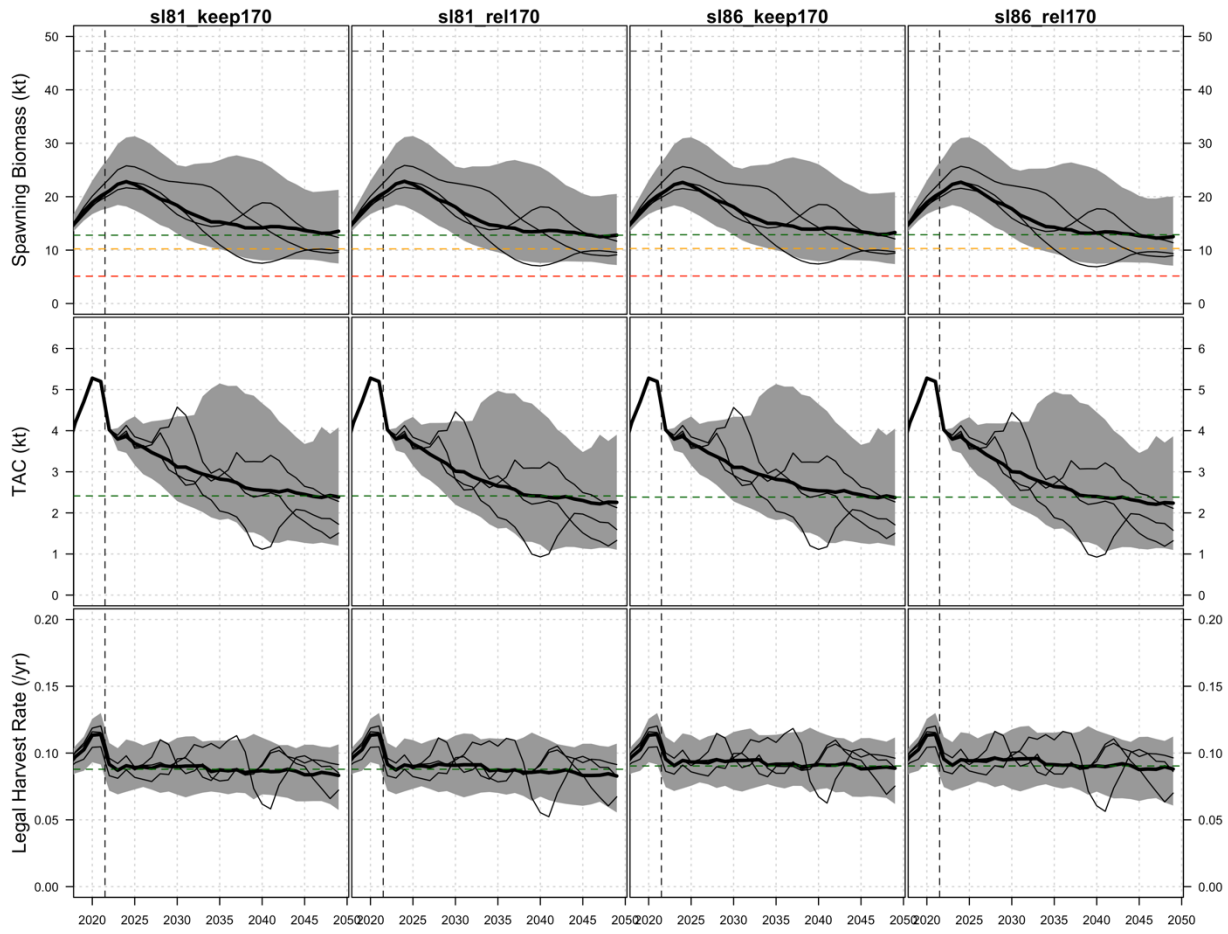

Figure 26. Simulation envelopes for spawning biomass (top row), total allowable catch (TAC, middle row), and realised fishing mortality rate (bottom row) for 2022 – 2050 under stratified random survey with the rampedFmsy harvest control rule. Envelopes represent the central 95% (grey) of outcomes, median (50% above/below; thick black line), and spaghetti traces (thin lines) showing 3 randomly chosen example outcomes. Horizontal dashed reference lines show B_{MSY} (top, green), 0.8 B_{MSY} (top, yellow), and the limit reference point of 0.4 B_{MSY} (top, red), MSY (middle, green), and legal U_{MSY} (bottom).

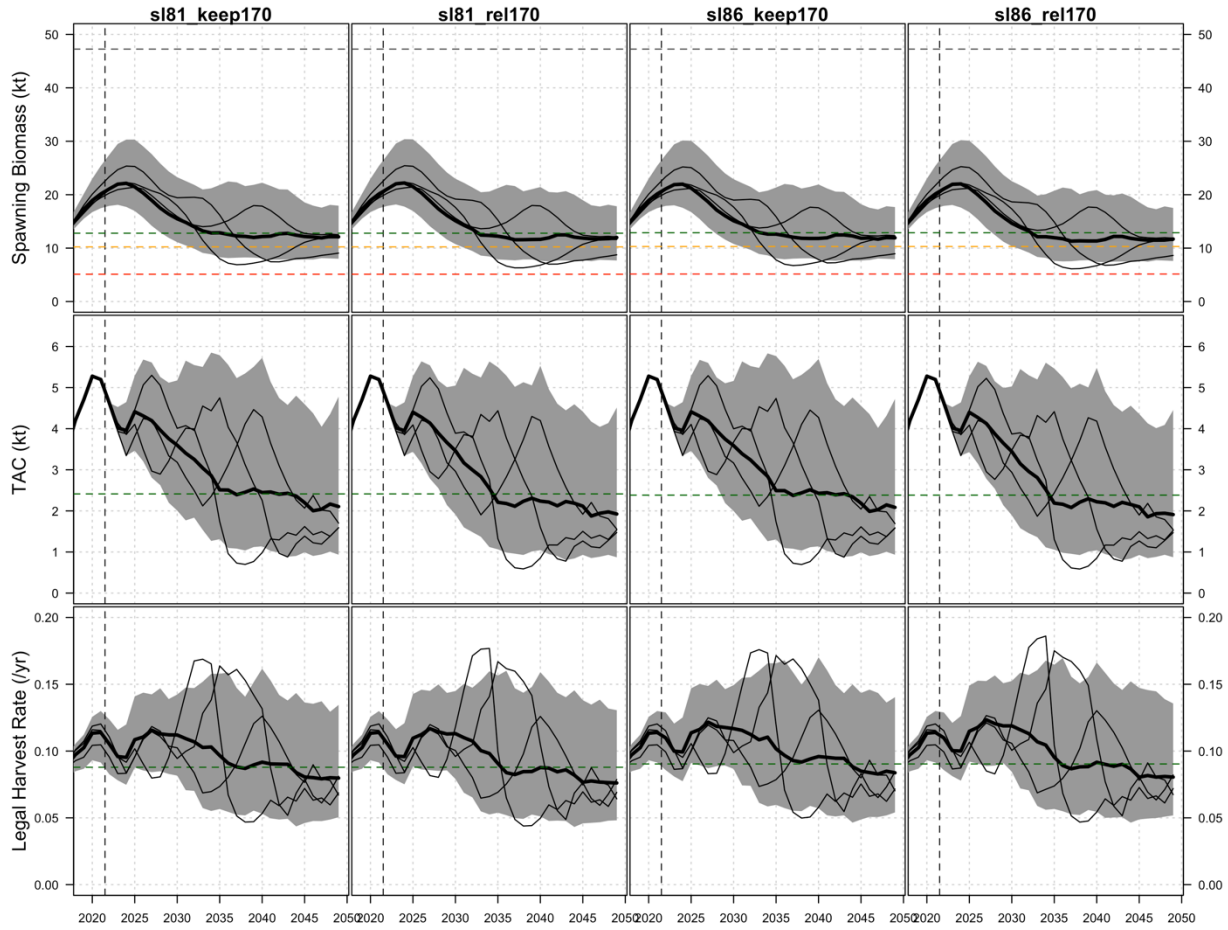

Figure 27. Simulation envelopes for spawning biomass (top row), total allowable catch (TAC, middle row), and realised fishing mortality rate (bottom row) for 2022 – 2050 under fixed station survey with the artic1.2Fmsy harvest control rule. Envelopes represent the central 95% (grey) of outcomes, median (50% above/below; thick black line), and spaghetti traces (thin lines) showing 3 randomly chosen example outcomes. Horizontal dashed reference lines show B_{MSY} (top, green), 0.8 B_{MSY} (top, yellow), and the limit reference point of 0.4 B_{MSY} (top, red), MSY (middle, green), and legal U_{MSY} (bottom).

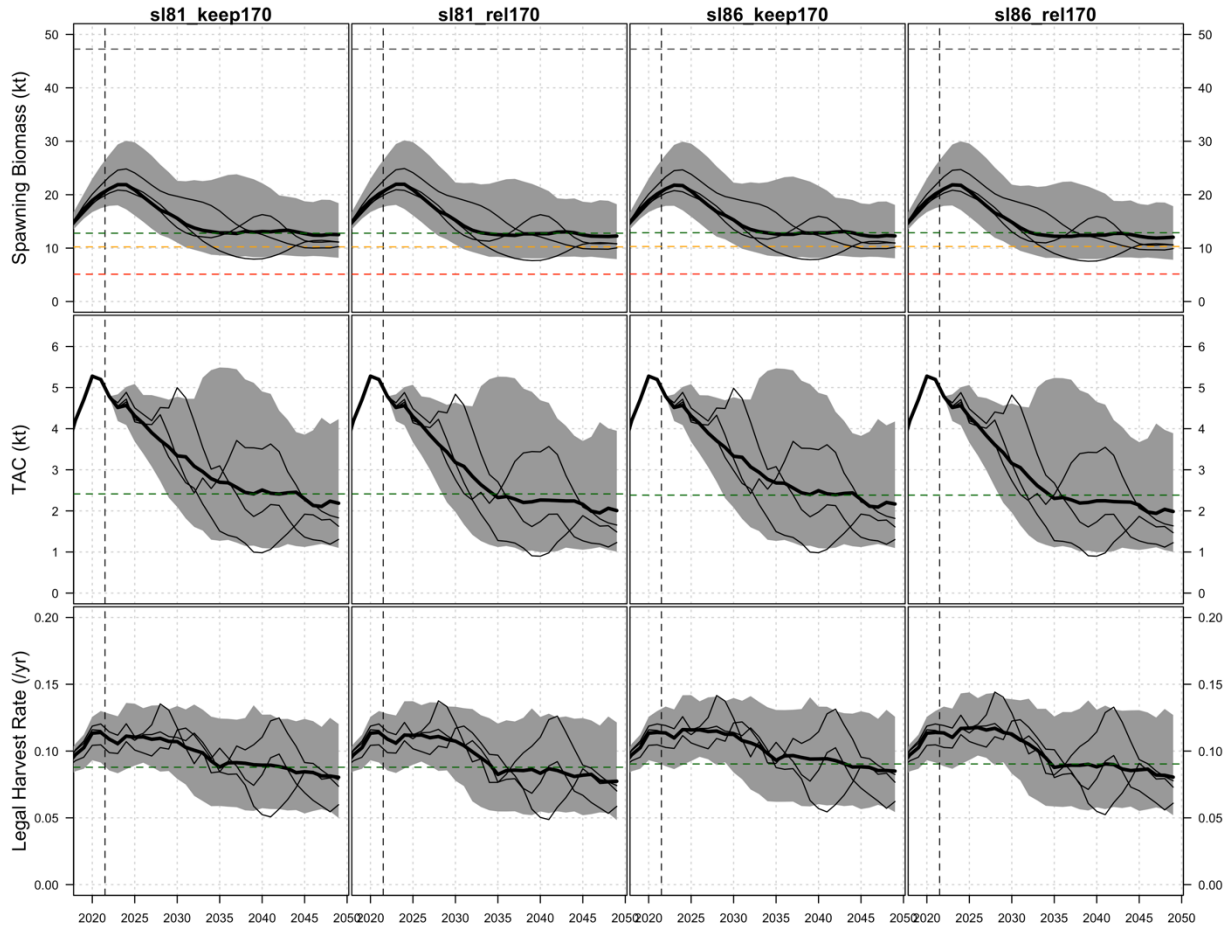

Figure 28. Simulation envelopes for spawning biomass (top row), total allowable catch (TAC, middle row), and realised fishing mortality rate (bottom row) for 2022 – 2050 under the stratified random survey with the artic1.2Fmsy harvest control rule. Envelopes represent the central 95% (grey) of outcomes, median (50% above/below; thick black line), and spaghetti traces (thin lines) showing 3 randomly chosen example outcomes. Horizontal dashed reference lines show B_{MSY} (top, green), 0.8 B_{MSY} (top, yellow), and the limit reference point of 0.4 B_{MSY} (top, red), MSY (middle, green), and legal U_{MSY} (bottom).

APPENDIX A

NAFO AREA 3 RV SURVEY DATA

At the request of reviewers following the November Atlantic Halibut framework CSAS review, the Newfoundland (NAFO area 3) NLRV survey indices and catch-at-length data were included in the SISCAL data set.

The SISCAL model is fit to the NLRV survey data using the same model structure as for the Maritimes Summer Ecosystem Research Vessel Survey, with a conditional MLE of observation residual standard error and survey catchability. The Newfoundland survey was also assumed to have dome-shaped selectivity, with the same functional form and parameter prior distribution as the 4VWX survey.

The model converged and posteriors were sampled with no issues. There was a slight scale increase, with unfished biomass around 17 kt higher than the model without the NLRV data presented in the main body of this document. However, despite the difference in scale, current stock status, recruitments, and harvest rates were all similar to the model without NLRV data (Figure A.1).

While the SISCAL-AH model fits to NLRV catch-at-length compositions were acceptable (Figure A.2), the fit to NLRV survey indices of abundance was not acceptable for conditioning the operating model for Atlantic Halibut closed-loop simulations (Figure A.3). The NLRV index increases 5-fold from the mid-late 2000s to its peak, while over the same period the RV_4VWX survey increases only by around 3 fold. We attempted to weight each data point's contribution to the likelihood by NLRV survey CVs as well, but there was no improvement in the fit.

Given the mismatch between the two RV survey trends, and the inability to fit both RV survey indices with a single-area model, the process producing large NLRV survey indices is not being captured in the SISCAL-AH model structure. We recommend further research examining the reasons why NLRV index is increasing more rapidly, and adjustments to the model structure (e.g., spatial components) before including this index in operating model.

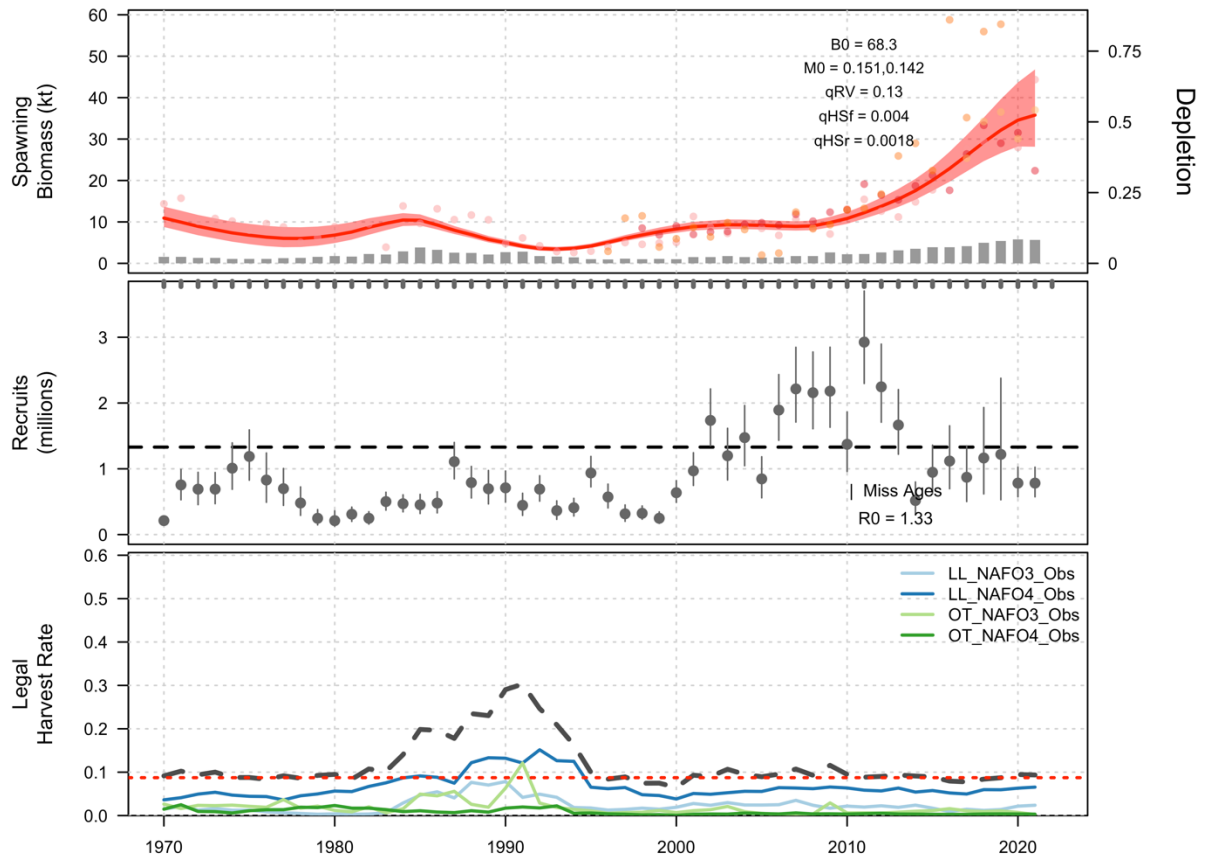

Figure A.1. Posterior spawning biomass (top), recruitment (middle) and legal harvest rates (bottom) for Atlantic Halibut, estimated by the SISCAL model when fit to all data including the NLRV survey indices and catch-at-length.

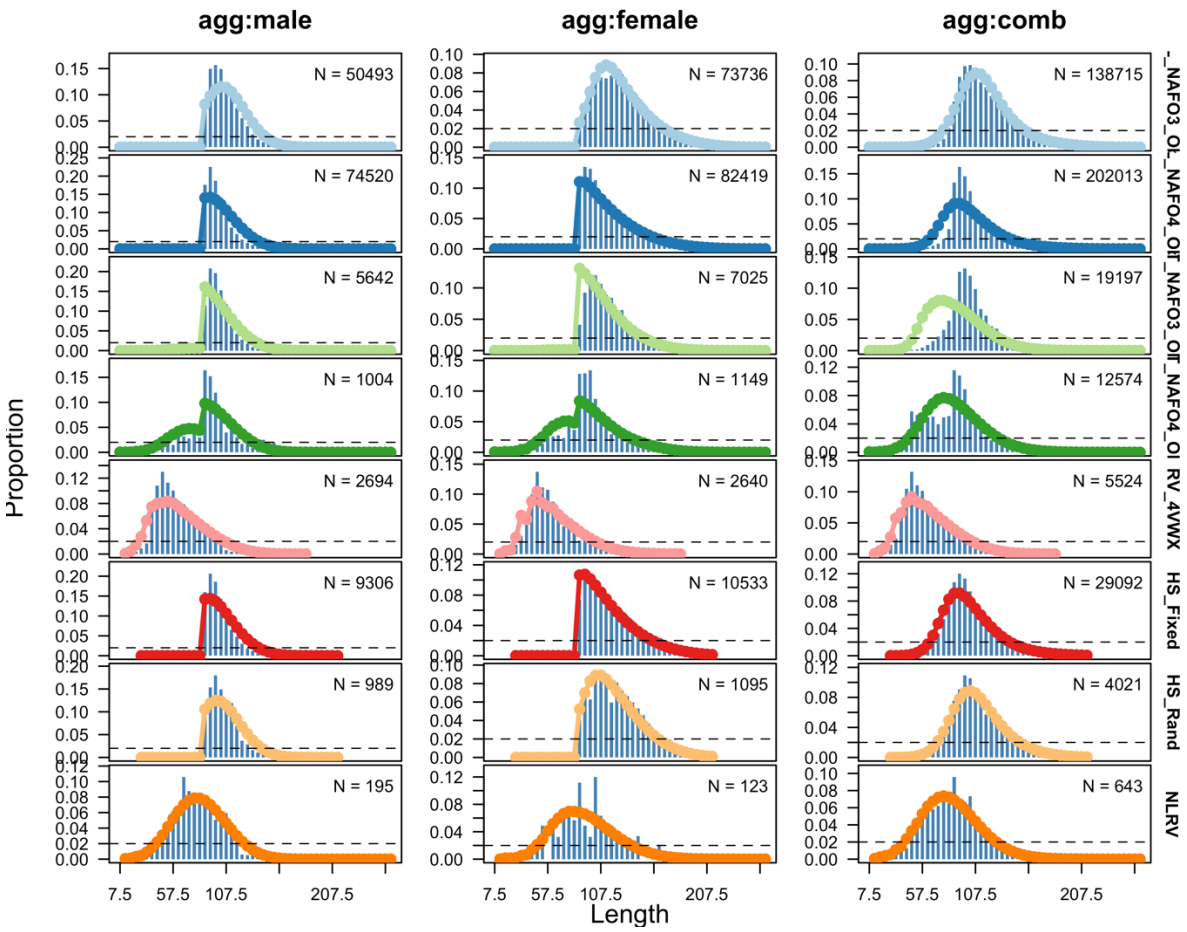

Figure A.2. Time-averaged catch-at-length data and expected catch-at-length in the SISCAL model when fit to the NLRV survey index and catch-at-length data.

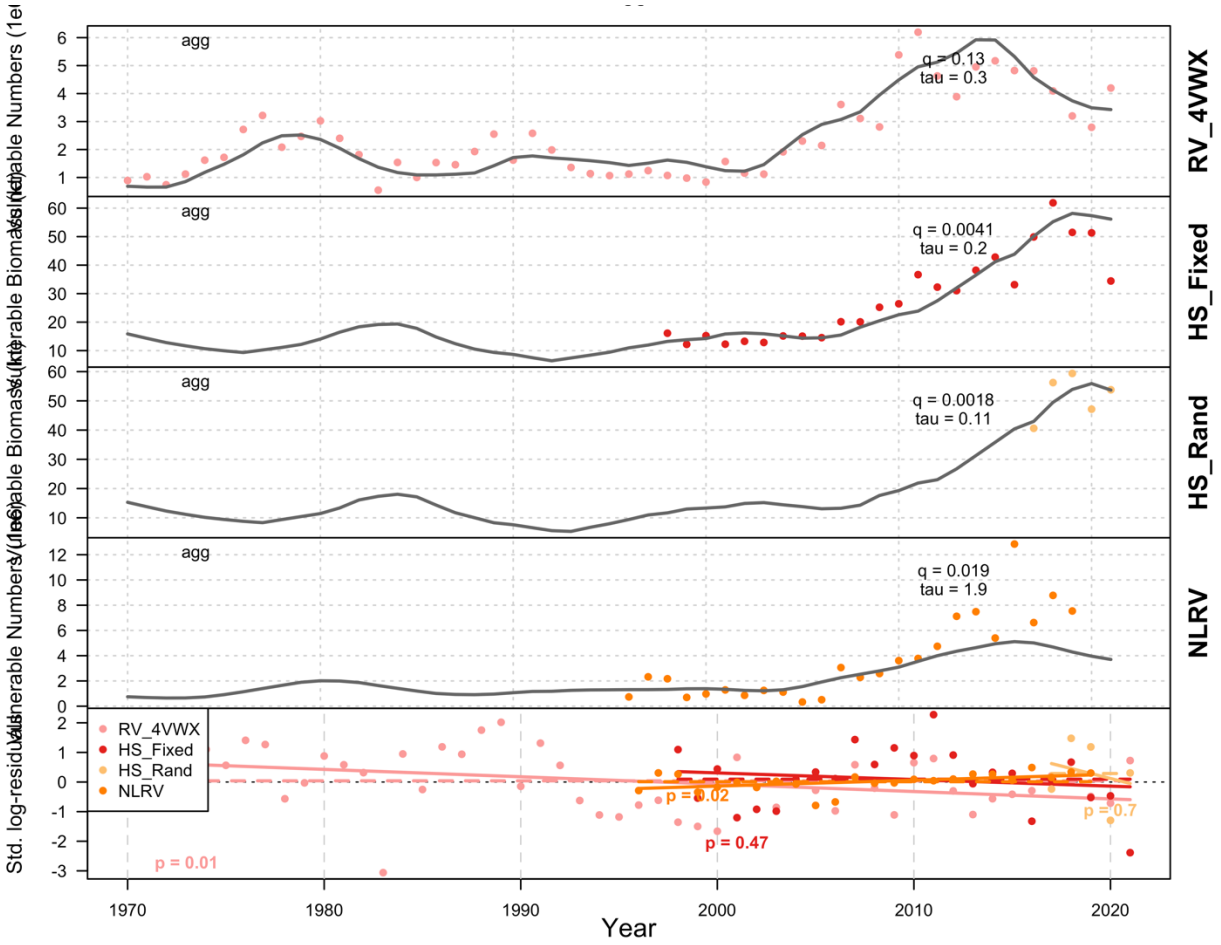

Figure A.3. SISCAL-AH fits to survey indices. Points show indices scaled by survey catchability, while lines show modeled vulnerable states (biomass for HS surveys, and numbers for RV surveys). The bottom panel shows standardised log residuals for each survey, with a dashed line for the mean residual, and a solid line showing any residual trend with significance of the trend indicated by the p-value. Note the change in y axis for the bottom panel.

APPENDIX B

POSITIVE FECUNDITY-WEIGHT ALLOMETRY AND VOLUNTARY RELEASE OF LARGE HALIBUT

A set of alternative SISCAL operating model hypotheses were fit to Atlantic Halibut data under a range of Atlantic Halibut fecundity assumptions. A common assumption in fishery stock assessment modeling is that fecundity-at-age of individual spawners is directly related to body-weight (i.e., body cavity volume), and therefore has positive allometry with length, via a relationship of the form

$$f_a = \alpha W_a = \alpha c_1 L_a^{c_2},$$

where W_a is spawner weight-at-age in kg, α scales weight to eggs, and c_1, L, c_2 are the usual allometric length-weight relationship parameters (Table 5). This assumption means that the number of eggs per unit of body weight is the same for all spawners, implying that a unit of spawning biomass is equally productive as any other unit, regardless of the underlying age structure of the population.

For some large flatfish (e.g., Pacific Halibut) there is evidence of positive allometry in the fecundity-weight relationship (Schmitt and Skud 1978; Haug and Gulliksen 1988), where the fecundity-weight relationship takes the form

$$f_a = \alpha W_a^{\beta},$$

with $\beta > 1$ implying that larger spawners have more eggs per unit of body mass than smaller spawners. That is, positive allometry in the fecundity-weight relationship then implies that not all units of spawning biomass are equivalent, as a thousand tonnes of spawning biomass that is made up of large spawners produces more eggs than the same volume of younger or smaller spawners, which may then produce higher average recruitment.

OPERATING MODELS

We used the Haug and Gulliksen (1988) fecundity-weight model parameter $\alpha = 6.355$ (derived from a fecundity-at-length model, and defined a grid of β parameters from 1.0 – 1.5 in 0.1 increments. This grid contains both the positive allometry relationships found for Pacific Halibut (1.17, Schmitt and Skud 1978) and Atlantic Halibut (1.16, Haug and Gulliksen 1988). SISCAL was refit to the stock assessment data assuming the fecundity-at-age model

$$f_a = 6.355\, W_a^{\beta}$$

for every β value in the grid and replacing spawning biomass in the stock-recruitment relationship with the total number of eggs contained in all mature spawners. The resulting model estimates were then used to condition 6 ms3-HAL operating models (Table B.1). While there were increases in stock scale variables, like unfished biomass, unfished recruitment, and B_{MSY} and MSY, the optimal harvest rate U_{MSY} was unaffected by the fecundity model's allometry (Table B.1), implying that productivity was not affected by the fecundity model. Moreover, the effects of the fecundity model appear to be at the equilibrium level, as historical biomass is almost identical among all 6 fecundity hypotheses (Figure B.1)

MANAGEMENT PROCEDURES

Ten management procedures were tested under each fecundity scenario. The management procedures were all variations on the HSfix_rampedFmsy_sl81 procedure (explained in main text), corresponding to combinations of 5 discard mortality levels ranging from 0–1.25 times the

based model values in 0.25 increments, and 2 cases where 170+ cm halibut are either kept (keep170) or released with 80% probability (rel170). The management procedure names are a concatenation of the discard mortality multiplier, and the release procedure, i.e. dM0.75_keep170 is the procedure where discard mortality is multiplied by 0.75, and 170+ cm halibut are landed.

RESULTS

There did not appear to be a strong interaction between the level of positive allometry in the fecundity/weight relationship of halibut, and the release (and level of associated mortality) of 170+ cm fish. Over all three conservation metrics, the keep170 procedures, where large fish were landed, had better conservation performance than the rel170 procedures (Figure B.2). As fecundity increased, there were changes in the values of pHealthy, pTarget, and pOverfish for both keep170 and rel170 procedures, but the trends were similar for release behaviour and across the range of discard mortality rates. Similarities in the trend indicate that the underlying cause of differences may be based on the changes to model equilibria over the range of fecundity β parameter values, rather than any benefit derived from returning more fecund females back to the spawning stock. Indeed, while all metrics tend towards converging as β and the discard mortality decrease, there is never a point where the lines cross over (except for perhaps at $\beta = 1$, which is the lower limit of realism).

Table B.1. Unfished biomass, recruitment, and MSY based biological reference points for SISCAL-AH models fit under 6 fecundity allometry scenarios.

β	B_0	R_0	B_{MSY}	U_{MSY}	MSY
1.0	56.58	1.10	17.51	0.089	2.41
1.1	58.72	1.14	18.18	0.089	2.50
1.2	59.91	1.17	18.49	0.089	2.56
1.3	62.38	1.22	19.25	0.089	2.67
1.4	65.11	1.27	20.10	0.089	2.78
1.5	68.05	1.33	21.01	0.089	2.91

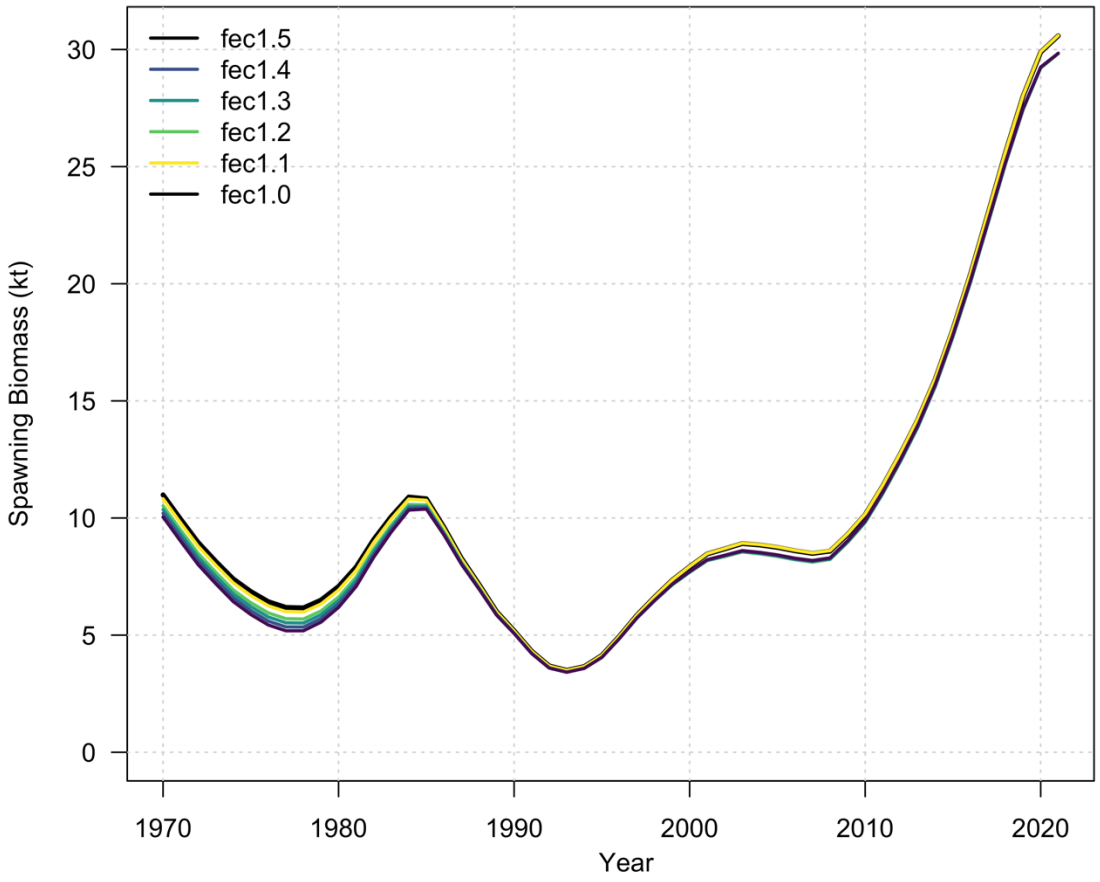

Figure B.1. SISCAL-AH model estimates of biomass under the 6 fecundity allometry hypotheses.

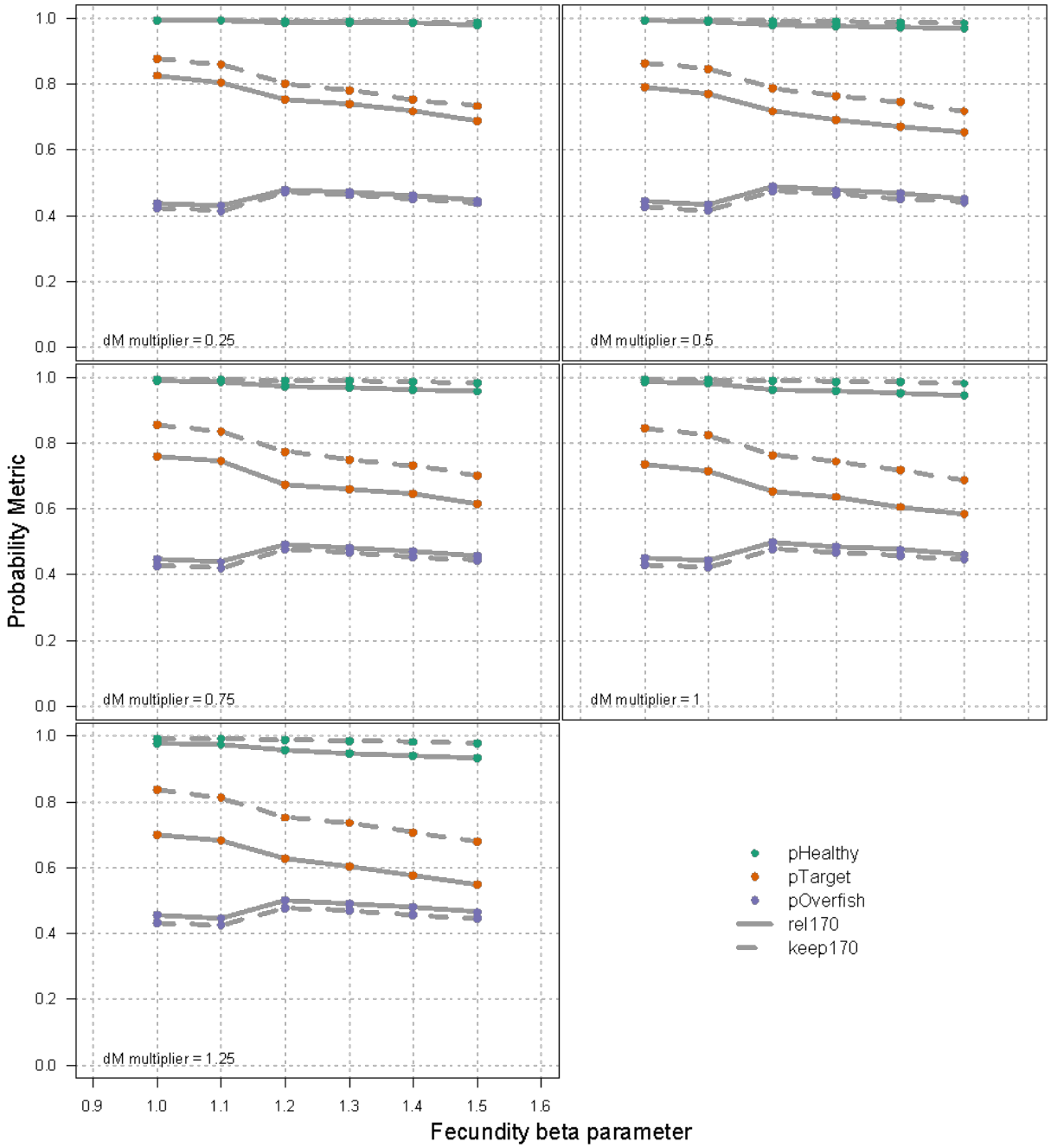

Figure B.2. Conservation performance metric responses to fecundity allometry values, releases of 170+ cm fish, and discard mortality rates.